REPUBLIC OF TURKEY
DOKUZ EYLUL UNIVERSITY
IZMIR INTERNATIONAL
BIOMEDICINE AND GENOME
INSTITUTE

INVESTIGATION OF THE ROLE OF WNT/β-CATENIN SIGNALING IN DEVELOPMENT OF ALZHEIMER'S DISEASE IN A ZEBRAFISH MODEL OF AMYLOID-β TOXICITY

MAKBULE DİLEK NAZLI

DEPARTMENT OF MOLECULAR BIOLOGY AND GENETICS

MASTER DISSERTATION

IZMIR-2022

THESIS CODE: DEU.HSI.MSc/2020850020

REPUBLIC OF TURKEY
DOKUZ EYLUL UNIVERSITY
IZMIR INTERNATIONAL
BIOMEDICINE AND GENOME
INSTITUTE

INVESTIGATION OF THE ROLE OF WNT/β-CATENIN SIGNALING IN DEVELOPMENT OF ALZHEIMER'S DISEASE IN A ZEBRAFISH MODEL OF AMYLOID-β TOXICITY

DEPARTMENT OF MOLECULAR BIOLOGY AND GENETICS

MASTER DISSERTATION

MAKBULE DİLEK NAZLI

Assoc. Prof. Dr. Güneş ÖZHAN

(This thesis is supported by TUBITAK 2210-C Domestic Graduate Scholarship Program for Priority Areas)

THESIS CODE: DEU.HSI.MSc/202085002

T.C.
DOKUZ EYLÜL ÜNİVERSİTESİ
İZMİR ULUSLARARASI BİYOTIP VE GENOM ENSTİTÜSÜ

ÇEVRİM İÇİ YÜKSEK LİSANS TEZ SAVUNMA SINAVI TUTANAĞI

Dokuz Eylül Üniversitesi İzmir Uluslararası Biyotıp ve Genom Enstitüsü Genom Bilimleri ve Moleküler Biyoteknoloji Anabilim Dalı Molekküler Biyoloji ve Genetik Yüksek Lisans Programı 2020850020 numaralı öğrencisi Makbule Dilek NAZLI, "INVESTIGATION OF THE ROLE OF WNT/β-CATENIN SIGNALING IN DEVELOPMENT OF ALZHEIMER'S DISEASES IN A ZEBRAFISH MODEL OF AMYLOID-β TOXICITY" konulu Yüksek Lisans tezini 03/08/2022 tarihinde saat: 13.00 'da çevrim içi ortamda yapılan savunma sınavı sonucunda başarılı olmuştur.

BAŞKAN

Doç. Dr. Günçe ÖZHAN

JÜRİ ÜYESİ

Dr. Öğr. Üyesi Yavuz OKTAY

JÜRİ ÜYESİ

Yrd. Doç Dr. Adil ŞEYTANOĞLU

Sınavın Yapılışında Uygulanan Yöntem

☒ Çevrim İçi

☒ Sınav kayıt altına alınmıştır.

TABLE OF CONTENTS

LIST OF TABLES

LIST OF FIGURES

ABBREVIATIONS

CNS ..... Central Nervous System

EGFP .....Enhanced Green Fluorescent Protein

GFAP ..... Glial Fibrillary Acidic Protein

GSK-3β .....Glycogen Synthase Kinase 3 beta

Neurod1.....Neurogenic Differentiation Factor 1

PCNA ..... Proliferating Cell Nuclear Antigen

S100β .....S100 Calcium-Binding Protein β

TCF .....T-Cell Factor

Aβ42……...Amyloid Beta-42

BACE ..... Beta Secretase

PSEN1……Presenilin-1

PSEN2……Presenilin-2

APPA .....Amyloid Precursor Protein-A

APPB..... Amyloid Precursor Protein-B

C-Caspase3……..Cleaved Caspase-3

rpl13..... Ribosomal Protein L13

P-β-catenin .....Phospho-β-catenin

ACKNOWLEDGEMENTS

I would like to express my deepest gratitude to my supervisor Assoc. Prof. Dr. Güneş Özhan, who just like her name was born into my life like the "Sun" in the darkest moment of my journey. She thrusted out her hand to me, helped me to find myself and trusted me no matter what.

I would like to thank,

My dear lab partner Yusuf Kaan Poyraz, who taught me everything he knows when I came to the laboratory, and who wholeheartedly wanted me to be included in the Alzheimer's team,

To my dear teammate Doğaç İpekgil, who undertook all the experimental work when I had to write a thesis and was my biggest supporter in the laboratory,

To my dear teammate Ebru Turhanlar Şahin, who took all the brain sections so that I could get the excellent brain images available in my thesis,

To dear Dr. Yağmur Azbazdar, who we consulted for her knowledge on every subject we did not know in the laboratory and who never turned us down and all Özhan Lab members who supported me.

I would like to thank my dear family Sevda Eren, Ali Nazlı, Sevinç Nazlı, and Daisy Nazlı for their full support in everything I have succeeded and failed to achieve.

And finally, at the age of 21, for being my second advisor in academic life from the first moment I walked through the lab door for my internship, for making me the greatest warrior alive, for bringing me to the surface every time I hit bottom, and for believing in me even when I didn't believe in myself, my companion I would like to express my deepest gratitude to Dr. Ali Uyan.

This thesis was supported by TUBITAK 2210-C Domestic Priority Areas Graduate Scholarship Program.

INVESTIGATION OF THE ROLE OF WNT/β-CATENIN SIGNALING IN DEVELOPMENT OF ALZHEIMER'S DISEASE IN A ZEBRAFISH MODEL OF AMYLOID-β TOXICITY

ABSTRACT

The Wnt/β-catenin signal transduction pathway is evolutionarily conserved and plays a key role in the regulation of development in the embryonic period, synapse formation in adulthood, apoptosis, and adipogenesis. Due to its pleiotropic and basic function, an abnormal activation or disruption in this signaling pathway may be associated with many diseases such as Alzheimer's, cancer, diabetes, and Parkinson's.

Alzheimer's disease (AD) is a neurological disease characterized by dementia and loss of synaptic functions and associated with aging. Alzheimer's disease is characterized by three distinctive pathologies: (1) accumulation of extracellular beta-amyloid plaques, (2) accumulation of intracellular Tau clusters, and (3) diffuse cell death seen in advanced Alzheimer's disease. However, synapse losses that can be seen in the early course of the disease represent the most common pathological link of the disease and are the most important cause of cognitive losses. Current animal models suggest that this synapse degeneration and loss is triggered by accumulating Aβ oligomers. Intercellular accumulation of this oligomer, which is very important for synaptic stabilization and function, causes deregulation of Wnt signaling pathways. This deregulation of the Wnt signaling pathway triggers synapse degeneration and leads to damping in synapse functions. This disruption in the signaling pathway is a trigger for the further progression of AD.

In the scope of the thesis, Alzheimer's disease, which can be triggered by the Aβ42 peptide, was modeled using adult transgenic (6XTCF) zebrafish. Zebrafish have genes orthologous to some human genes thought to play an important role in Alzheimer's disease. Throughout the thesis, Aβ42 was injected into the brains of adult zebrafish using the CVMI technique, and a model of Alzheimer's disease was created. The regenerative response of zebrafish to toxicity was analyzed by qPCR and confocal microscopy.

The change in AD pathogenesis was investigated in zebrafish treated with IWR-1 drug on days of high regeneration. As a result, more Aβ accumulation and cell loss were observed in zebrafish treated with IWR-1.

Key Words: WNT/β-CATENIN, Zebrafish, Alzheimer’s Disease

ALZHEIMER HASTALIĞI GELİŞİMİNDE WNT/B-KATENİN SİNYAL İLETİMİNİN ROLÜNÜN ZEBRA BALIĞI AMİLOİD-B TOKSİSİTE MODELİNDE ARAŞTIRILMASI

ÖZET

Wnt/β-katenin sinyal iletim yolu evrimsel olarak korunur ve embriyonik dönemde gelişimin düzenlenmesinde, yetişkinlikte sinaps oluşumunda, apoptozda ve adipogenezde anahtar rol oynar. Pleiotropik ve temel işlevi nedeniyle, bu sinyal yolundaki anormal bir aktivasyon veya bozulma, Alzheimer, kanser, diyabet ve Parkinson gibi birçok hastalıkla ilişkilendirilebilir.

Alzheimer hastalığı (AH), demans ve sinaptik fonksiyonların kaybı ile karakterize ve yaşlanma ile ilişkili nörolojik bir hastalıktır. Alzheimer hastalığı üç farklı patoloji ile karakterize edilir: (1) hücre dışı beta-amiloid plaklarının birikmesi, (2) hücre içi Tau kümelerinin birikmesi ve (3) ileri Alzheimer hastalığında görülen yaygın hücre ölümü. Ancak hastalığın erken seyrinde görülebilen sinaps kayıpları, hastalığın en yaygın patolojik bağlantısını temsil eder ve bilişsel kayıpların en önemli nedenidir. Mevcut hayvan modelleri, bu sinaps dejenerasyonu ve kaybının, amiloid-beta (Aβ) oligomerlerinin birikmesiyle tetiklendiğini ileri sürmektedir. Sinaptik stabilizasyon ve fonksiyon için çok önemli olan bu oligomerin hücreler arası birikimi, Wnt sinyal yollarının deregülasyonuna neden olur. Wnt sinyal yolunun bu deregülasyonu sinaps dejenerasyonunu tetikler ve sinaps fonksiyonlarında sönümlemeye yol açar. Sinyal yolundaki bu bozulma, AH'nın daha da ilerlemesi için bir tetikleyicidir.

Tez kapsamında, Aβ42 peptidi tarafından tetiklenebilen Alzheimer hastalığı, yetişkin transgenik (6XTCF) zebra balığı kullanılarak modellenmiştir. Zebra balığı, Alzheimer hastalığında önemli bir rol oynadığı düşünülen bazı insan genlerine ortolog genlere sahiptir. Tez boyunca, CVMI tekniği kullanılarak yetişkin zebra balıklarının beyinlerine Aβ42 enjekte edildi ve bir Alzheimer hastalığı modeli oluşturuldu. Zebra balıklarının toksisiteye karşı rejeneratif tepkisi, qPCR ve konfokal mikroskopi ile analiz edildi.

AD patogenezindeki değişiklik, yüksek rejenerasyon günlerinde IWR-1 ilacı ile tedavi edilen zebra balıklarında araştırıldı. Sonuç olarak, IWR-1 ile tedavi edilen zebra balıklarında daha fazla Aβ birikimi ve hücre kaybı gözlendi.

Anahtar Sözcükler: Wnt/β-katenin sinyal iletim yolu, zebra balığı, Alzheimer hastalığı.

1. INTRODUCTION AND AIM

Alzheimer's disease (AD) has been associated with disruptions in Wnt/β-catenin signaling activity in many previous studies. Despite dozens of studies, its pathophysiology is still unknown; For this reason, new treatment methods that can cure the disease or stop the progression of symptoms cannot be found. Since AD is an irreversible disease, no results could be obtained from AD models created with mammals with low regenerative capacity. This led to the need for a new platform to model the disease.

This study aims to demonstrate the activation and role of Wnt/β-catenin signaling in various stages of disease formation and changes in the brain during Alzheimer's disease, apoptosis, and neurogenesis by modeling Alzheimer's disease with Aβ42 toxicity to be induced by using Aβ42 in the adult zebrafish brain.

The hypothesis of this study includes that the deregulation of the Wnt/β-catenin signaling pathway in Alzheimer's disease further triggers the progression of the disease.

1.1. General Information

1.1.1 Alzheimer's Disease

Dementia is a syndrome defined as the loss of cognitive functions of the brain caused by an injury or disease in the brain (Arvanitakis et al., 2019). The most common cause of dementia is Alzheimer's disease (AD), accounting for approximately 60 to 80% of all dementia cases (Barker et al., 2002). AD ranks 6th among causes of death with an estimated prevalence of approximately 30 million people worldwide. The age of the individual is the most important risk factor for AD, with an exponential increase in prevalence from 3% to 32% between the ages of 65 and 85 years. AD is a chronic neurodegenerative disease characterized histopathologically by the presence of amyloid-β (Aβ) peptides in extracellular senile plaques and the formation of intracellular neurofibrillary tangles (NFTs) composed of the hyperphosphorylated, microtubule-associated protein tau (Serrano-Pozo et al., 2011; Jack Jr. et al., 2018).

Insights into the pathogenesis of AD arose from the pioneering neuropathological observations of senile plaques and NFYs by Alois Alzheimer (Hippius & Neundörfer, 2003), and 80 years later it was discovered that these plaques are composed of a 39-43-amino acid peptide now known as Aβ (Glenner et al., 1984). Aβ is derived from the sequential cleavage of amyloid-β precursor protein (APP) by β-secretase and γ-secretase, resulting in C- and N-terminal cleavage

and/or modification to yield 2 major isoforms. These isoforms are Aβ40 and Aβ42. Aβ42 is the more amyloidogenic and precipitates first. The precipitated amyloid betas diffuse and form plaques (Figure 1).

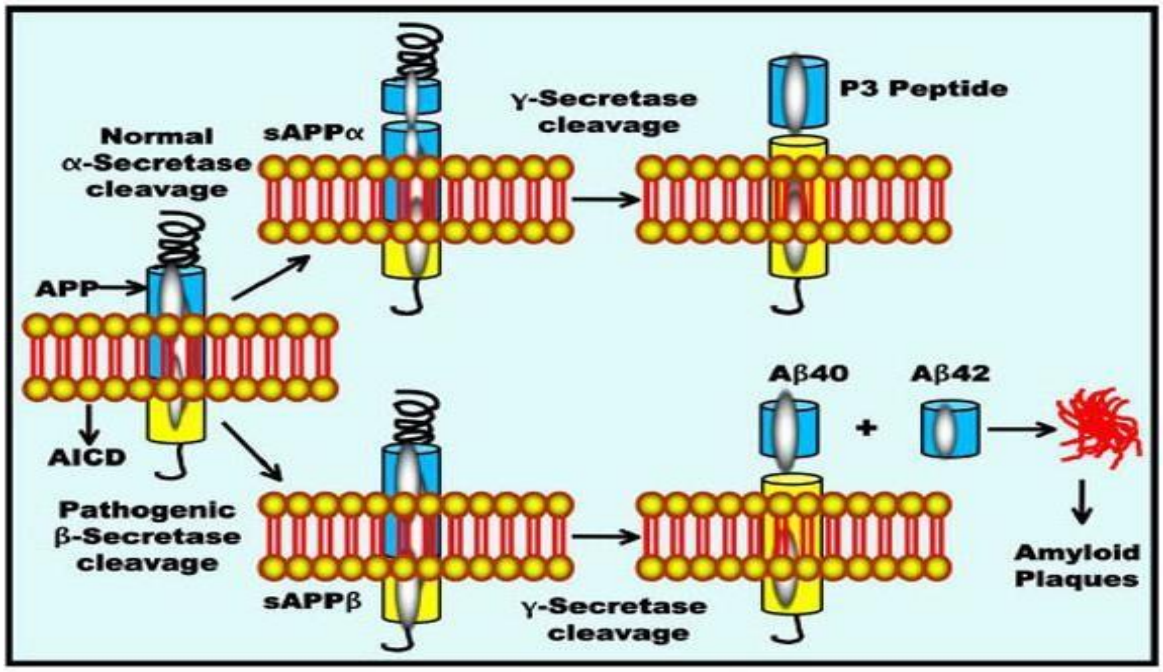

Figure 1: Processing of App and Aβ formation *(adapted from* Kumari & Heese, 2010)

According to the amyloid hypothesis of AD, the accumulation of Aβ peptides as senile plaques in the brain with aging is the main feature in the pathogenesis of AD, due to both increased production and decreased clearance of plaques. Senile plaques are surrounded by activated microglia and reactive astrocytes, which are associated with neuronal degeneration; are extracellular deposits consisting of the Aβ peptide in the center (Selkoe & Hardy, 2016; Heckmann et al., 2019). The accumulation of Aβ causes mitochondrial dysfunction, inflammation, and oxidative stress that impair neuronal homeostasis, as well as decrease neuroplasticity and neurogenesis, hyperphosphorylation of Tau protein, and apoptosis (Figure 2).

Current information about the molecular pathogenesis and physiology of AD comes largely from understanding the distinctive neuropathologies. However, there is no treatment available yet to stop the progression of the disease. treatment approaches are aimed at relieving symptoms and reversing synaptic levels.

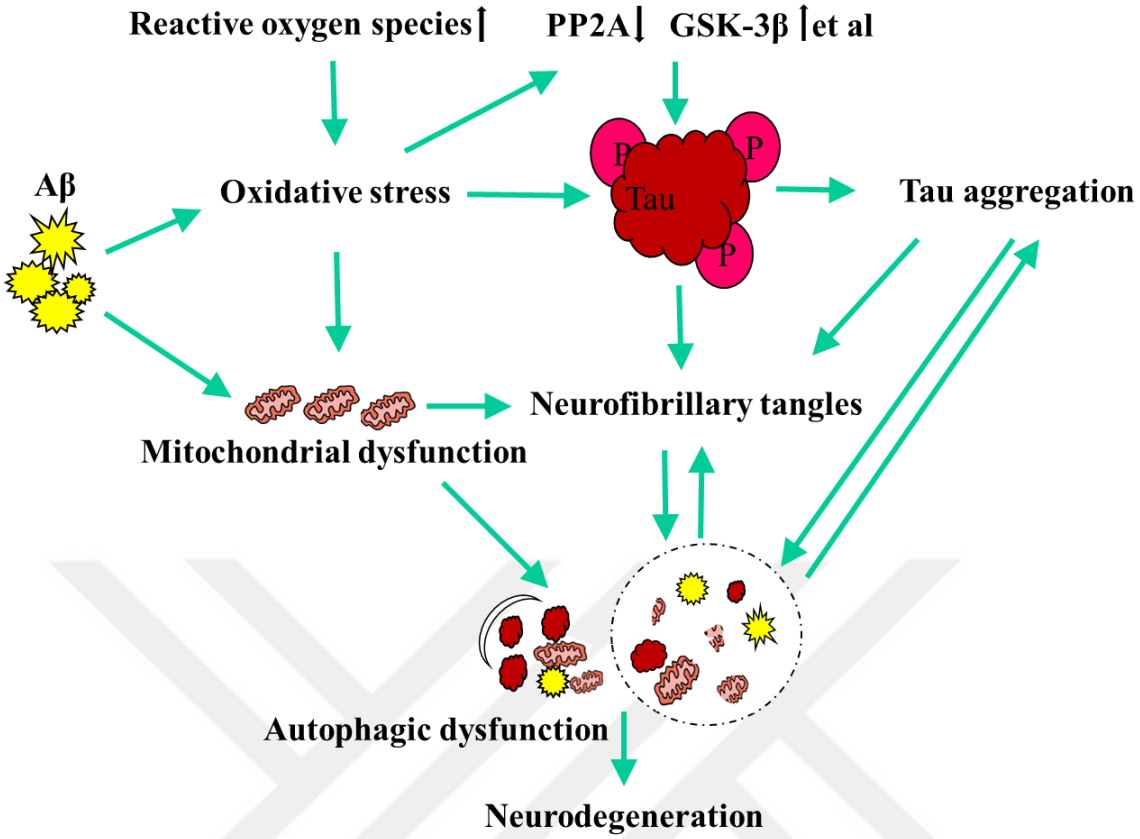

Figure 2: Neurodegeneration and cell death in AD (*adapted from* Liu et al., 2015).

The mechanisms by which tau can spread by increasing the bioactivity of microglia in the presence of amyloid-beta have been described in previous studies (Zhang et al., 2019). They trigger the oligodendrocytes near soluble amyloid-beta, causing the release of cytokines. These released cytokines activate microglia, causing tau to be taken into the cell and become more bioactive.

Studies to stop the progression of the disease are generally aimed at reducing the level of Aβ accumulated in the brain or preventing this accumulation. In this context, although reducing Aβ production by inhibiting β-secretase and γ-secretase activities seems to be an appropriate strategy, in the mouse amyloidosis model, BACE1 inhibition could not prevent the growth of existing plaques, although BACE1 inhibition limited the formation of new plaques (Peters et al., 2018). There are many BACE1 inhibitors in the clinical research phase and ongoing studies (Panza et al., 2018; Egan et al., 2019; Henley et al., 2019; Lopez et al., 2019). γ-secretase inhibitors have also been used in clinical studies, and studies have been terminated due to dose-limiting side effects, low drug Efficacy, or worsening of cognitive functions (Doody et al., 2014; Coric et al., 2015).

Another approach to reducing amyloid accumulation is γ-secretase modulators, which alter the profile of secreted Aβ peptides by modifying the processivity of the enzyme without inhibiting γ-secretase activity (Golde et al., 2013; Wagner et al., 2017). Despite all these important efforts and advances by the scientific world to understand pathobiology, no treatment method has proven effective in humans yet to stop the progression of the disease and to regress although genetic and biochemical analyzes, in vitro and in vivo studies, and imaging data clearly role of Aβ aggregation in the onset of AD, the most important reason for the lack of successful results from clinical studies is the unknown mechanisms of emergence and progression of the disease. The most important signaling pathway that emerges in this context and is associated with AD is the Wnt beta-catenin signaling pathway. (Ng et al., 2019).

1.1.2 Wnt Signaling Pathway

The Wnt beta-catenin signaling pathway is a family of proteins that perform critical cellular functions such as cell division, organogenesis, and stem cell regeneration. Signaling within the cell is divided into beta-catenin-dependent and beta-catenin-independent. A disruption in signal transmission plays a critical role in the development of many diseases such as cardiovascular problems, cancer, diabetes, and Alzheimer's Disease.

1.1.2.1 Canonical Wnt/β-Catenin Signaling Pathway

The canonical WNT signaling pathway, which was first identified in the intracellular signaling pathway and has been highly conserved in the evolutionary process, is seen as the most important signal transduction pathway among the existing Wnt signaling pathways. At the same time, this pathway is beta-catenin-dependent, where beta-catenin moves from the cytoplasm to the nucleus of the cell and functions as a transcriptional regulator in the regulation of intercellular adhesion.

In the absence of Wnt ligands, the Dikkoppf family (DKK1-4) binds to any of the transmembrane receptors (Fzd, LRP5-6) thus preventing Wnt ligand binding. Wnt inhibitory factor (WIF-1) and Fzd receptors (SFRP1-5) bind the WNT ligand to themselves, preventing the ligand from interacting with the receptors. When Wnt is inactive, β-catenin is phosphorylated and binds to the complex of adenomatous polyposis coli (APC), scaffold protein (AXIN), glycogen synthesis kinase (GSK3β), and casein kinase (CK1). With the addition of the protein containing the β-transducin repeat, which is included in the complex

structure, β-catenin leaves the complex and goes to the proteasome and is degraded by the ubiquitination method. Therefore, the stability of β-catenin depends on the complexation of Axin, AC,a GS K-3β with CK1. Since β-catenin is degraded in the cytoplasm, the signal does not reach the nucleus, so gene expression cannot occur (Figure 3a).

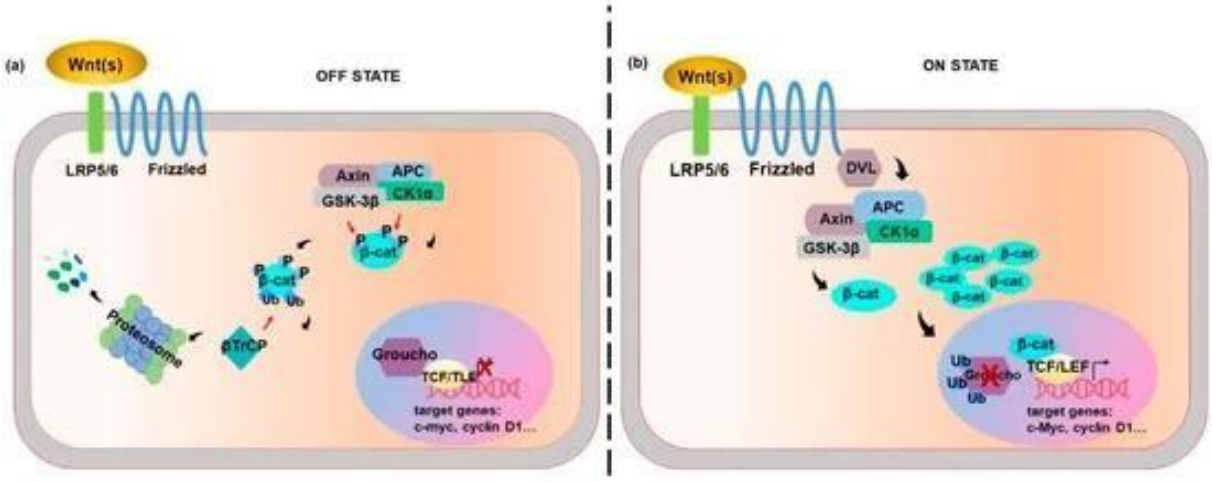

Figure 3: Canonical WNT/ β-Catenin Signaling Pathway (*adapted from* Coni et al., 2020)

For the signaling pathway to be activated, Wnt ligands must bind to Frizzled receptors and establish an LRP5/6 relationship. Thus, the activated β-catenin takes on a stable structure. GSK3β and CK1 kinases phosphorylate LRP5/6. DVL molecules also bind to FZD receptors and interact with LRP5/6, attaching the phosphatephosphatetein to itself and deactivating the proteosome. β -catenin, which is free in the cytoplasm, is also freed from fragmentation. As a result, the accumulated β-catenin is transported to the cell nucleus and mediates the expression of T cell factor and lymphoid enhancing factor (TCF/LEF) target genes (Figure 3b).

1.1.2.2 Wnt Signaling and Alzheimer's Disease

The Wnt/β-catenin signal transduction pathway is tightly controlled by numerous positive and negative regulators. Some of the well-characterized Wnt pathway components and regulators, such as the Wnt antagonist dkk1 and the β-catenin degradation complex component axin2, also tatargetsnd are under transcriptional control of the pathway (Jho et al., 2002; Gonzalez-Sancho et al., 2005). Dkk1 inhibits canonical Wnt signaling by interacting with the Lrp5/6 coreceptor (Niehrs, 2006). Dkk1 was found to be highly expressed in the brains of Alzheimer's patients in mouse AD models (Caricasole et al., 2004; Rosi et al., 2010). In parallel, increased Gsk3ß activity, Lrp6 polymorphism, and reduced Wnt signaling activity due to the splicing variant, and cytoplasmic ß-catenin levels were found in the brains of patients (Zhang et al., 1998; Pei et

al., 1999; De Ferrari et al., 2007; Alarcón et al., 2013; Kawamura et al., 2020). Mass spectrometric analysis of samples obtained from patients' brains also supports the decrease and deterioration in canonical Wnt signal transmission (Elliott et al., 2018; Xu et al., 2019; Bai et al., 2020).

To summarize, Aß-derived and Dkk-mediated dysregulated Wnt/β-catenin signaling activity is a prominent feature associated with impaired synaptic integrity and cognitive decline in AD. The mechanisms of this possible connection revealed both at the molecular and cellular level during disease manifestation and repair are of great importance for the treatment of the disease.

1.1.3 Alzheimer's Disease and Current Animal Models

Despite the complex nature of the disease, most experimental studies of AD pathogenesis have used mouse models with mutant forms of the APP and PSEN genes to recapitulate autosomal dominant familial AD (La Ferla et al., 2007), which accounts for less than 1% of human AD cases. These aggressive mutations, when introduced into rodents, resulting in the accumulation of age-related Aβ plaques. However, cognitive impairment is usually mild and/or variable with minor neurodegeneration, and mice do not develop human-like NFTs, which are all key clinicopathological features of the human condition (La Ferla & Green, 2012). Mice carrying tau mutations associated with human primary tauopathies have also been developed. Although these mice display significantly abnormal tau in the brain, it does not fully recapitulate AD tauopathy, even when the mice are crossed with APP-transgenic mice (Kitazawa et al., 2012).

Reduced clearance rather than overproduction of Aβ appears to be the driver of Aβ accumulation in the commonly occurring late-onset form of AD (Mawuenyega et al., 2010). In addition, clinical trials of inhibitors of β-secretase and γ-secretase attempting to reduce amyloid have been ineffective and have even exacerbated AD in humans (Karran et al., 2011). Thus, AD, as it occurs in humans, is more complex than the pathology modeled in rodents genetically engineered to overproduce human sequence Aβ. The inability to obtain results from these animal models may be because they only model a part of AD pathology and do not include common co-occurring disorders such as vascular disease and other proteinopathies, tauopathy, synucleinopathy, TDP-43 proteinopathy, etc.).

1.1.4 Zebrafish as a Model Organism

Since its phylogenetic proximity to humans, zebrafish has recently been recognized as a reliable

model for studies of behavior, neural circuitry, and neurodegenerative disease (Guo, 2004). CoA (Coenzyme A) comparison of zebrafish brain structure with humans shows that basic brain organization (Mueller et al., 1996) is highly conserved, with similar key neuroanatomical (Mueller & Wullimann., 2009; Rink et al., 2004) and neurochemical pathways related to human disease. The organization of the zebrafish brain is similar to that of other vertebrates, with the presence of structures of the lateral pallium (located in the telencephalon) despite smaller cerebral hemispheres and the structure and function of the optic tectum, with similarly defined areas such as the hypothalamus and olfactory bulb. The zebrafish and mammalian encephalon share many structural features such as major organization (anterior, mid, and hindbrain including diencephalon, telencephalon, and cerebellum) or major neurotransmitter systems (Mueller et al., 2004). It has been shown that the main neurotransmitter circuits such as glutamatergic (stimulant) and GABAergic (inhibitory) exist in the zebrafish brain (Rico et al., 2011). In addition to major excitatory and inhibitory neurotransmitters, muscarinic cholinergic receptors have been confirmed in brain extracts of adult zebrafish by radioligand binding methods (Park et al., 2008). In addition, neurotransmitters such as GABA, dopamine, serotonin, histamine, glutamate, and acetylcholine are also found in zebrafish (Panula et al., 2006). In addition, zebrafish CNS, microglia (Peri & Nusslein-Volhard., 2008) oligodendrocytes and myelin (Avila et al., 2007; Yoshida & Maclin., 2005) cerebellar Purkinje cells (Koulen et al., 2000), motor neurons It also includes the cellular types found in the mammalian brain, such as (Westerfield et al., 1986) or astrocytes (Kawai et al., 2001).

1.1.4.1 Adult Neurogenesis in Zebrafish

The reason for the existence and number of regions with neurogenic capacity varies in different vertebrates examined until now is still elusive. While zebrafish can continue to grow as adults, they have several different progenitor regions in the brain that reproduce continuously during homeostasis and contribute to zebrafish growth throughout life.

The adult mammalian brain has very little capacity to repair damage to neurons. Neurogenesis can only occur through stem cells found in some regions. This situation requires the use of another platform for new therapeutic approaches to be developed. Unlike adult mammals, the adult zebrafish brain can produce new neurons continuously throughout its life, thanks to its neural stem cells located in a total of 16 different regions. Little is known about the signal transduction pathways and their molecular mechanisms that are active in zebrafish brain

regeneration, which can be triggered by non-traumatic pathways such as disease. At this point, it is of great importance to examine the signaling pathways that come into play, especially in the early and late stages of disease formation (Alvarez-Buylla et al., 2001; Kriegstein & Alvarez-Buylla, 2009; Bonfanti & Peretto, 2011).

2. MATERIALS AND METHODS

2.1. Type of the Study

The type of research carried out in this study is experimental.

2.2. Time and Place of Study

All experiments were carried out in İzmir Biomedicine and Genome Center between October 2020-July 2022.

2.3. Materials of Study

2.3.1 Zebrafish Handling and Maintenance

Wild Type zebrafish were used to validate the model at the beginning of the study. WIK strains are used as a WT. Subsequently, the transgenic zebrafish line Tg(6XTCF:d2EGFP) (for short 6XTCF), a reporter of Tcf/Lef-mediated transcriptions been shown to precisely detect Wnt/β-catenin pathway activity in various cellular contexts, was used to reveal whether Wnt/β-catenin signaling is activated (Shimizu et al., 2012). Zebrafish were maintained under standard conditions in the IBG aquarium system and a 12-hour dark and 12-hour light cycle at 28ºC was followed.

2.3.2 Primers

The primers used for qPCR were designed in PrimerQuest and synthesized by Oligomer Biotechnology in Ankara. Primers delivered in lyophilized form were dissolved in Nuclease Free Water (NFW).

Table 1: List of primers

Name of Primers	Forward Primers (5'->3')	Reverse Primers (3'->5')
D2EGFP	TATCATGGCCGACAAGCAGA	CTGGTAGTGGTCGGCGAG
IL-1B	GCTGGAGATCCAAACGGATA	ATACGCGGTGCTGATAAACC
GFAP	ACCCGTGACGGAGAGATCAT	GCCAGTGTCTGAGCCTCATT
PCNA	CAAGGAGGATGAAGCGGTAACA	CTGCGGACATGCTAAGTGTG
APPA	CGAGAACGAACACGCTCACT	CTGGATCACGGCCTTCTTGT
APPB	TCGATGAGCAAGACACCAGT	CTGGAGCTTCCAGGTAACGA
PSEN1	GGCTCATCCTCGCTGCTATT	TCCACAAGGATTCGCAGAGG
PSEN2	GGCTCATCCTCGCTGCTATT	TCCACAAGGATTCGCAAGAGG
BACE	GGAGCCGGATACAACCACAA	CATAGTACCACTCTCGGCGG
HUC	ATCACCTCACGCATCCTG	TTGTTGGCGAACTTTACG
HUD	GGCCTATGGCGTTAAGAGGTTC	CCAGCCTGTTCCTGTGTGAC

2.3.3 Kits and Enzymes

Table 2: List of kits and enzymes

Kit/Enzyme	Vendor	Cat. No.
miRnNeasy Mini Kit	QIAGEN	217004
Iscript cDNA Synthesis Kit	Bio-rad	1708891

2.3.4 Consumables

The specified consumables were used during the thesis.

Table 3: List of consumables

2ml Eppendorf Tubes
1,5 ml Eppendorf Tubes
Glass Bottle
96 well plate
Disposable Pipette Tips
Embedding Molds
Needle (30G 0.3x13mm)
Disposable Microtome Blades

2.3.5 Chemicals

Table 4: List of chemicals

Chemical	Vendor	Cat. No
Dimethyl Sulfoxide (DMSO)	Sigma-Aldrich	472301
Ethanol Absolute	Merck	1.00986
Ethylenediaminetetraacetic acid (EDTA)	Sigma-Aldrich	E6635
Gelatin	Merck	G1393
Glycerol	Amresco	0854-1L
IWR-1	Sigma-Aldrich	I0161
Methanol	Sigma-Aldrich	32213
Paraformaldehyde	Sigma-Aldrich	158127
Potassium Chloride	Sigma-Aldrich	P9541
Sodium Chloride	Sigma-Aldrich	S9898
Sodium Phosphate dibasic	Sigma-Aldrich	255793
Sodium Phosphate monobasic	Sigma-Aldrich	S0751
Sucrose	Sigma-Aldrich	S0389
Tissue-Tek O.C.T	SAKURA	4583
Tricaine	Sigma-Aldrich	E10521
Tris	Sigma-Aldrich	252859
Triton X-100	Sigma Aldrich	T8787
Chloroform	Merck	1.02431

2.3.6 Instruments

The devices used during this thesis work are listed below.

Table 5: List of instruments

Instruments	Vendor
Vortex	Thermo Fisher Scientific
Microwave Oven	Beko
Borosilicate Glass Capillary	World Precision Instrument
7500 Real-Time PCR-ABI 7500 FAST	Applied Biosystem
Cryostat	LEICA
LSM880 Laser Scanning Confocal Microscopy	ZEISS
Nanodrop 2000 Spectrophotometer	Thermo Fisher Scientific
pH meter	Mettler Toledo
Thermal Cycler	Thermo Fisher Scientific
Power Supply	Bio-rad
mySPIN 6 Mini Centrifuge	Thermo Fisher Scientific

2.4. Data Collection Methods

2.4.1 Preparation of Amyloid Beta Peptide

Amyloid beta peptide received by Peptiteam in lyophilized form was dissolved in acetonitrile:dimethylformamide: distilled water at a ratio of 1:1:1. The dissolved Amyloid beta was diluted to 40 micromolar with PBS.

2.4.2 Establishment of an adult zebrafish Alzheimer's model based on amyloid beta toxicity

Adult zebrafish with a length of 25-32 mm were injected into the zebrafish brain using the CVMI method, with 40µM and 2µl of Amyloid beta peptide for each fish, which we determined in our previous studies. Fish were anesthetized with Tricaine (Tricaine methanesulfonate, MS-222, Sigma-Aldrich) before injection. The fish were taken into clean water immediately after the injection. The waters were refreshed daily.

2.4.3 Validation of an adult zebrafish Alzheimer's Model based on Amyloid beta

To confirm the toxicity from Aβ42 of to investigate the regenerative response of zebrafish to it, analyzes were carried out at various stages from the 1st day to the 14th day after injection. In addition, for the control of Aβ42 plaques in the brain, immunofluorescence staining was performed with anti-Aβ42 antibody in brain sections taken.

2.4.4 RNA isolation

RNA isolation was performed with the Qiagen-RNeasy Micro Kit. The dissected telencephalons were taken into 1.5-gauge sterile Eppendorf, then 50 microliters of QIAzol Lysis Buffer were added and homogenized, and another 650 microliters of Qiazol were added. After adding 150ul chloroform to each tube, it is mixed for 2 minutes and centrifuged at 12.000 g for 15 minutes at +4 degrees. After centrifugation, the tube is divided into 3 parts and the upper part contains RNA. The upper part is transferred to another Eppendorf and 525µl of 100% ethanol is placed on it. Thoroughly mixed samples are transferred to collection tubes supplied by QIAGEN and centrifuged for 15 seconds at 8,000g at room temperature. Discard the flow-through and add 700µl RWT buffer on it and centrifuge again for 15 seconds at 8000g at room temperature.

Centrifuge (8000g, 15 seconds) is repeated by adding discard the flow through and 500µl of RPE buffer. Then 500µl 80% ethanol (prepared with nuclease-free water) is added and

centrifuged at 8000g for 2 minutes. At the end of the centrifugation, the columns are centrifuged at full

speed for 5 minutes with the lid open to dry the membrane, at the end they are centrifuged by adding nuclease-free water and the RNAs are transferred to the new tube.

2.4.5 cDNA Synthesis

The RNA samples obtained with 3.4.4 were prepared according to the protocol and then incubated in Thermal Cycler as shown in Table 6. It is stored at -20 until used.

Table 6: First and second steps of cDNA synthesis

First Step	
Component	Volume
RNA samples	Variable
Reverse Transcriptase	1µl
Nuclease Free Water	Variable
5x IScript Reaction Mix	4µl
Total Volume	20µl
Second Step	
Priming	5 min at 25℃
Reverse Transcription	20 min at 40℃
RT Inactivation	1 min at 95℃
Optional	Hold at 4℃

2.4.6 qPCR Analysis

Previously prepared cDNAs were diluted at 1:20 with nuclease-free water. GoTaq Master mix and Applied Biosystem 7500 Real-Time PCR thermal cycler were used for qPCR analysis. The reaction mix was prepared according to the following protocol (Table 7).

Table 7: Protocol for qPCR analysis

Components of qPCR Reaction Mix	**Volume**
Forward Primer	0,5µl
Reverse Primer	0,5µl
2X GoTaq Reaction Mix (with syber green)	5µl
cDNA	4µl
Total Volume	10µl

2.4.7 Tissue Preparation and Embedding

To preserve tissue integrity, dissected zebrafish heads are taken to Paraformaldehyde (PFA) immediately after dissection and treated with 4% PFA at +4 degrees for 2 days. After 2 days, it is transferred to 20% sucrose-20% EDTA solution. Zebrafish heads treated here for 2 days are taken into 30% Sucrose-20%Edta solution as the last step of decalcification and made ready for embedding after 2 days of treatment. The fixed tissue is embedding molds with 20% sucrose-7.5% gelatin solution and stored at -80 degrees until cryosectioning.

2.4.8 Cryosectioning

Cryosection of brain samples was performed with a cryostat (Leica) at -30°C, with the size of the sections 12 μm. Section samples taken were stored at -20°C until immunofluorescent staining on microscope slides (Fisherbrand-12550-17).

2.4.9 Immunohistochemistry and Imaging Process

The first day of the staining, brain samples stored at -20°C degrees are kept at room temperature for 20 minutes before staining. Afterward, all the steps below are applied and incubated in the primary antibody at +4°C degrees for one day (Table 8).

Table 8: Immunohistochemistry protocol

1X PBSTX	3x10 minutes
1X PBS	2x5 minutes
Sodium Citrate (ph:6)	15 minutes
1X PBS	2x5 minutes
1X PBSTX	2x10 minutes

Primary Antibody was applied at appropriate ratios (1:500) and kept wet and dark for 16 hours. On the second day of staining, brain samples kept in primary antibodies for 16 hours were washed in 3x10 PBSTX and then incubated with appropriate secondary antibodies for 2 hours at room temperature. After 10 minutes of DAPI application, slides were washed 3x5 minutes in PBS, and mounting was done. It was stored at +4°C until imaging. Z-stack images are collected with LSM 880 Laser scanning confocal microscopy (ZEISS) at 40X and 63X.

2.4.10 IWR Treatment

Aβ42-injected 6xTCF: D2EGFP transgenic fish were exposed to IWR-1 drug, which acts as a

Wnt/β-catenin inhibitor by stabilizing the Axin protein, starting 1 day before the days of high Wnt activity, and in this way, Wnt signaling activity was detected on the first and second half of the 14 days. It was inhibited on the 7th day. IWR-1 was added to the fish water at a concentration of 10μM, which we have shown to be effective before.

2.5. Study Plan and Calendar

Table 9: Study plan and calendar

Date Range	Experimental Studies
01 /12/2021-01/03/2021	Establishment of Alzheimer's Disease Model in Zebrafish
01/03/2021-01/07/2021	Validation of Alzheimer's Disease Model in Zebrafish
01/07/2021-01/12-2021	Investigation of the Role of Wnt/β-Catenin Signal Transmission Pathway in Regenerative Response from Alzheimer's Disease in Aβ Toxicity-Induced Alzheimer's Disease
01/12/2021-01/08/2022	Evaluation of Statistical Analysis of In Vivo Experiments

2.6. Data Evaluation

RT-qPCR results were analyzed with the unpaired student t-test and visualized with the Prism 8.0 Graphpad Program. Statistical significance is represented as *$p<0.05$; **$p<0.01$; ***$p<0.001$.

2.7. Limitation of Study

This study is limited to the outcome obtained from the zebrafish brain. Therefore, it would be proper to test the results in a mammalian system for further validation.

3. RESULTS

3.1. Establishment of an adult zebrafish AD model based on Aß neurotoxicity, molecular characterization of the model, and regenerative response

3.1.1 Determination of the effects of Aβ42 toxicity on the adult zebrafish brain

In order to observe the effects of Aβ42 toxicity on the brain and to validate the experimental model, RNA samples were collected from the WT adult zebrafish brain on the 1st, 3rd, 4th, 7th, and 14th days after injection. The expression of genes associated with amyloidogenesis is

known to increase in the brain under hypoxic conditions. Real-time quantitative PCR results to reveal the effect of toxicity induced in the zebrafish brain after Aβ42 injection on the expression of AD-related PSEN1, PSEN2, APPA, APPB and BACE1 genes are shown in Figure 4.

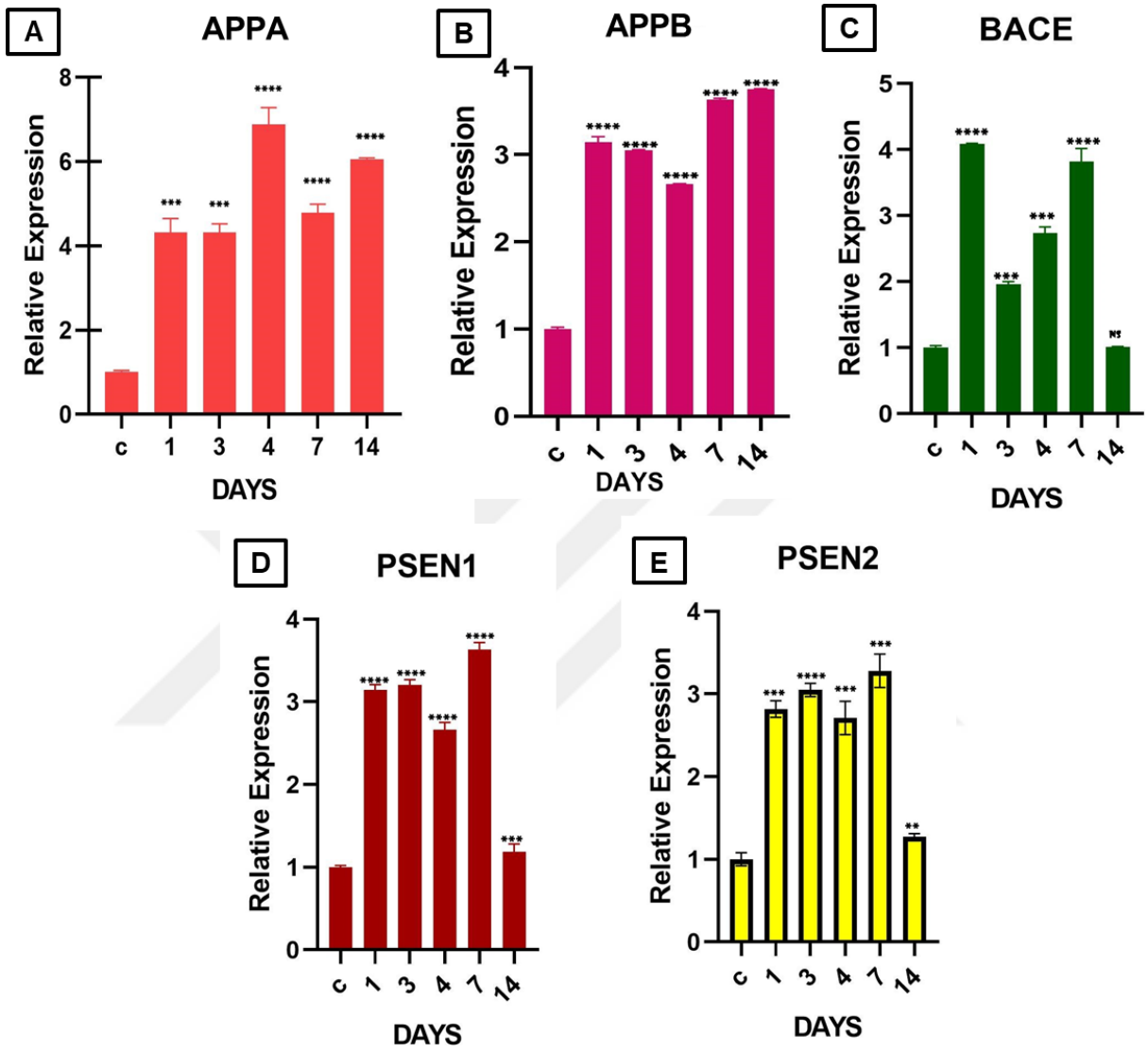

Figure 4: AD-related gene expression level (*rpl13* was used as endogenous control. The relative mRNA level was normalized to the corresponding *rpl13* mRNA expression. qPCR data presented here are means ± SD from triplicate data. Asterisk on individual bars represents a significant difference between the control group and NCP groups. Asterisks on half-tick-up lines represent a significant difference between the indicated groups. Student's unpaired t-test was used to calculate significance *P < 0.05, **P < 0.01, ***P < 0.001. Error bars indicate SEM. APPA (A), APPB (B), BACE (C), PSEN1 (D), and PSEN2 (E) gene expression levels compared to only PBS injected control group).

According to the results obtained in Figure 4A significant increase was observed in the expression of Alzheimer-related markers. A strong increase was observed in all genes on the 1st day of aβ42 injection, while a decrease was observed in the BACE (Figure 4C) gene on the

3rd day. Despite this decrease, the gene expression level is approximately 2 times higher than the control group without toxicity. On the 14th day, although the values of BACE, PSEN1, and PSEN2 genes approached the control group, they were still statistically significantly higher (Figure 4C/D/E)

Although the height of Alzheimer's genes observed in Figure 4 is a positive result for the formation of the model, immunofluorescence staining was performed with the anti-ab42 antibody on the same days to control the formation of aβ42 plaques.

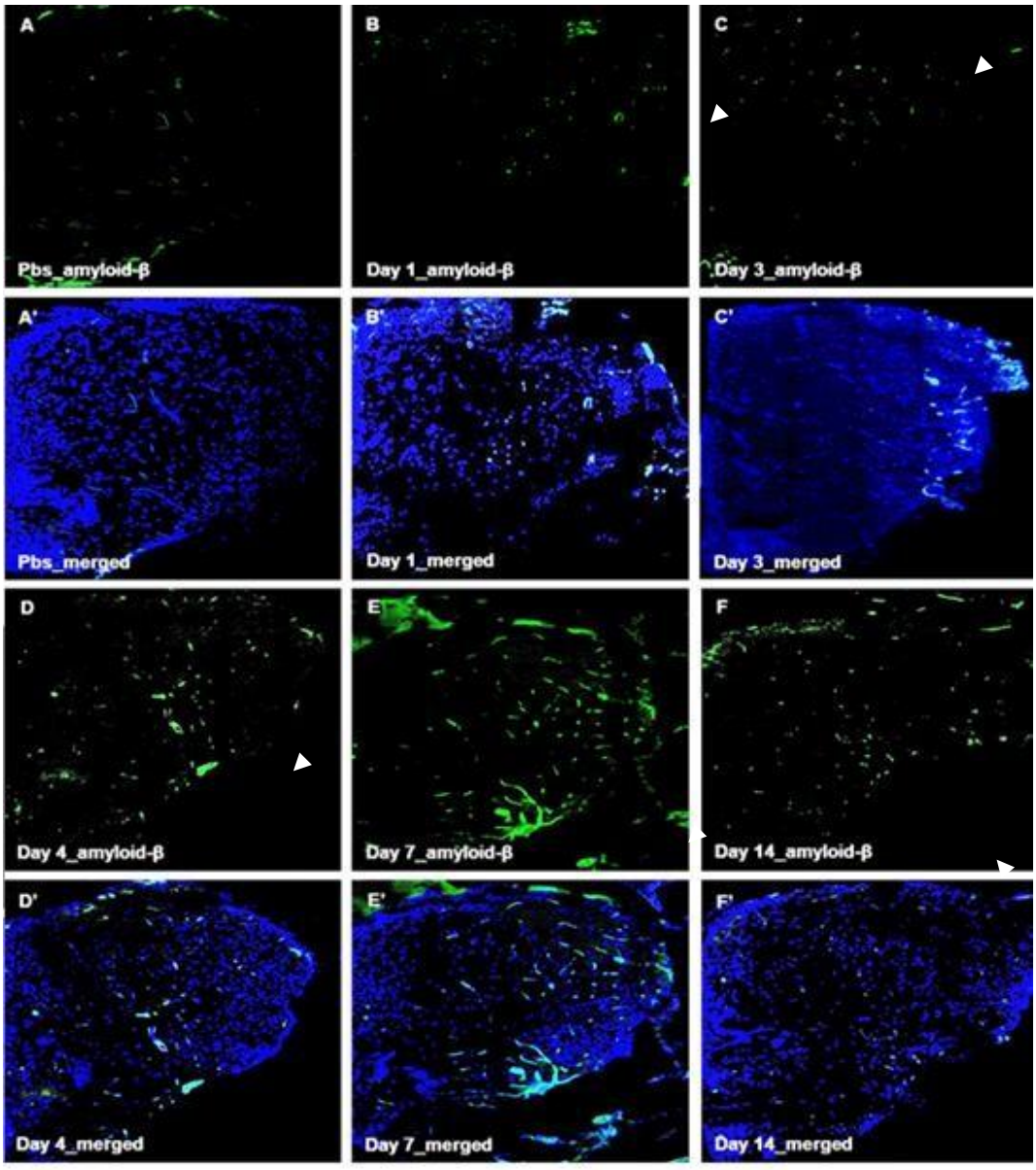

Figure 5: Immunofluorescence staining of Aβ plaques (Anti-Aβ42 immonostaining of brain section obtained from PBS (A), 1dpi (B), 3 dpi (C), 4dpi (D), 7dpi (E), 14dpi (F) A' , B' , C' , D', E', F' represent the DAPI staining. Scale bars 100µm).

The Aβ-42 plaques, which started to accumulate from day 1 of CVMI injection, generally accumulated between cells but were observed around blood vessels in some areas. While this accumulation showed that the model was formed successfully, it showed that the aβ42 toxicity observed on the 14th day was longer-lasting. On the other hand, the decrease in plaques seen on the 3rd day and the increase that became continuous after the 4th day is also compatible with the qPCR results.

3.1.2 Imaging of reactive gliosis and neurogenesis in Alzheimer's Disease caused by AB42 toxicity

Zebrafish brains provide activation of different brain cells to restore brain physiology in response to aβ accumulations leading to AD development and increasing radial glial cells in support of this process. In addition, recent studies have shown that PCNA has an important role not only in regulating the cell cycle but also in providing neuronal plasticity in patients with AD. To observe this process, PCNA and S100 staining were performed simultaneously on the brain sections taken and the PCNA gene expression level was checked by qPCR (Bronzuoli et al., 2016).

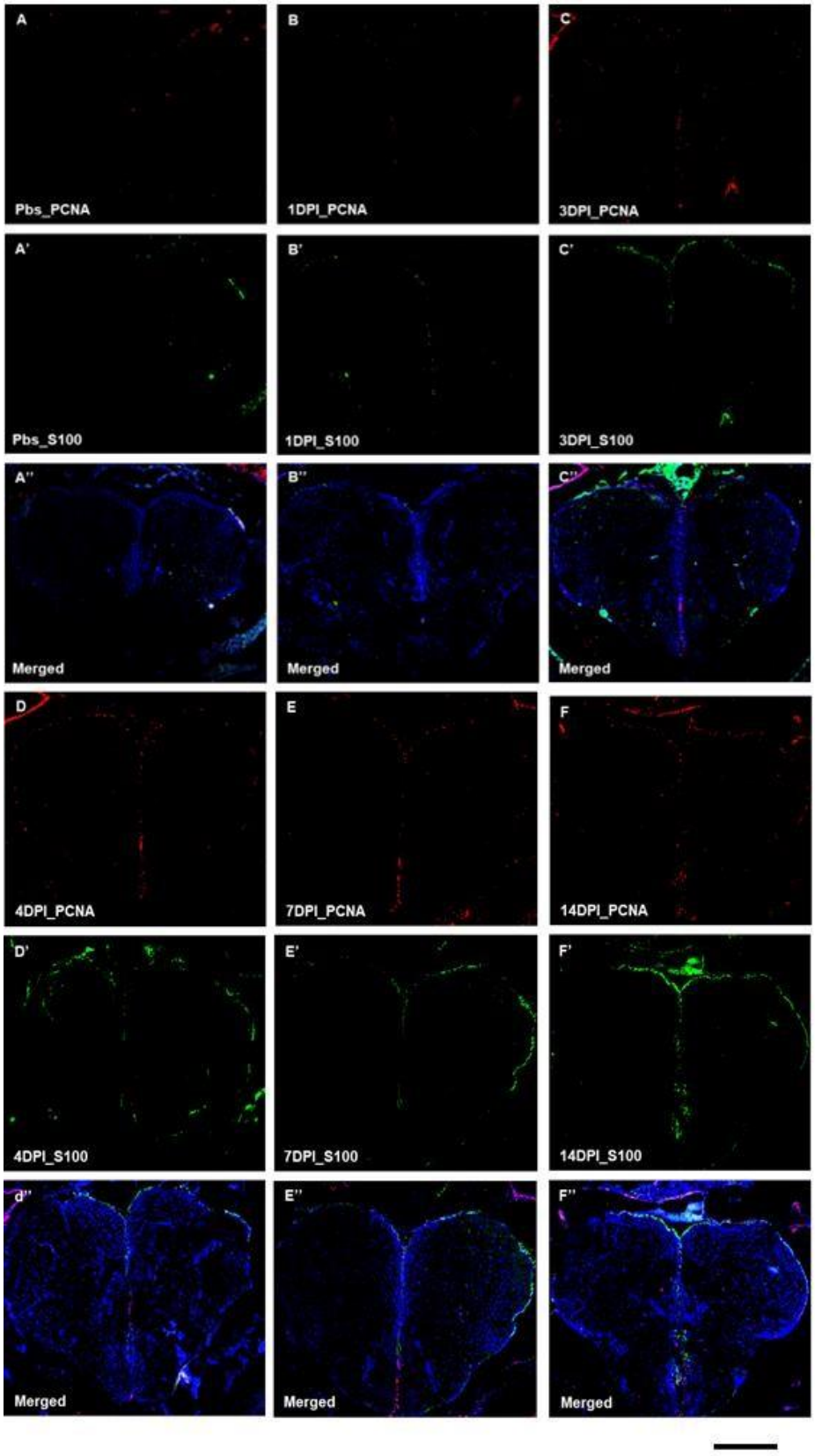

Figure 6: Anti-S100 and PCNA staining of brain sections that obtained from PBS (A,A'), 1dpi (B,B'), 3 dpi (C,C'), 4dpi (D,D'), 7dpi (E,E'), 14dpi (F, F'). Sections are counterstained for DAPI (A'', B'', C'' D'', E'', F''. Scale bars 100µm).

From the 1st day after the injection, it was observed that the adult zebrafish brain started reactive gliosis in the dorsal ventricular region and increased the s100 level. The adult zebrafish brain, which tried to provide homeostasis by increasing the proliferation of brain cells in the same region, slightly decreased on the 3rd day, and the S100 and PCNA levels were reactivated from the 7th day and continued until the 14th day. Relative expression levels of the PCNA gene seen in Figure 6 are also consistent with immunofluorescence staining, including the decrease on 3rd dpi.

In neurodegenerative diseases such as Alzheimer's disease, the speed of the astroglial response and the onset of reactive gliosis are evolutionarily conserved processes, and it expresses that the central nervous system is trying to fulfill its function. In addition, the increase in GFAP mRNA level has also been associated with Alzheimer's Disease (Diedrich et al., 1987). To test this hypothesis, real-time quantitative PCR and immunofluorescence staining were performed from mRNA samples taken from zebrafish telencephalon tissue.

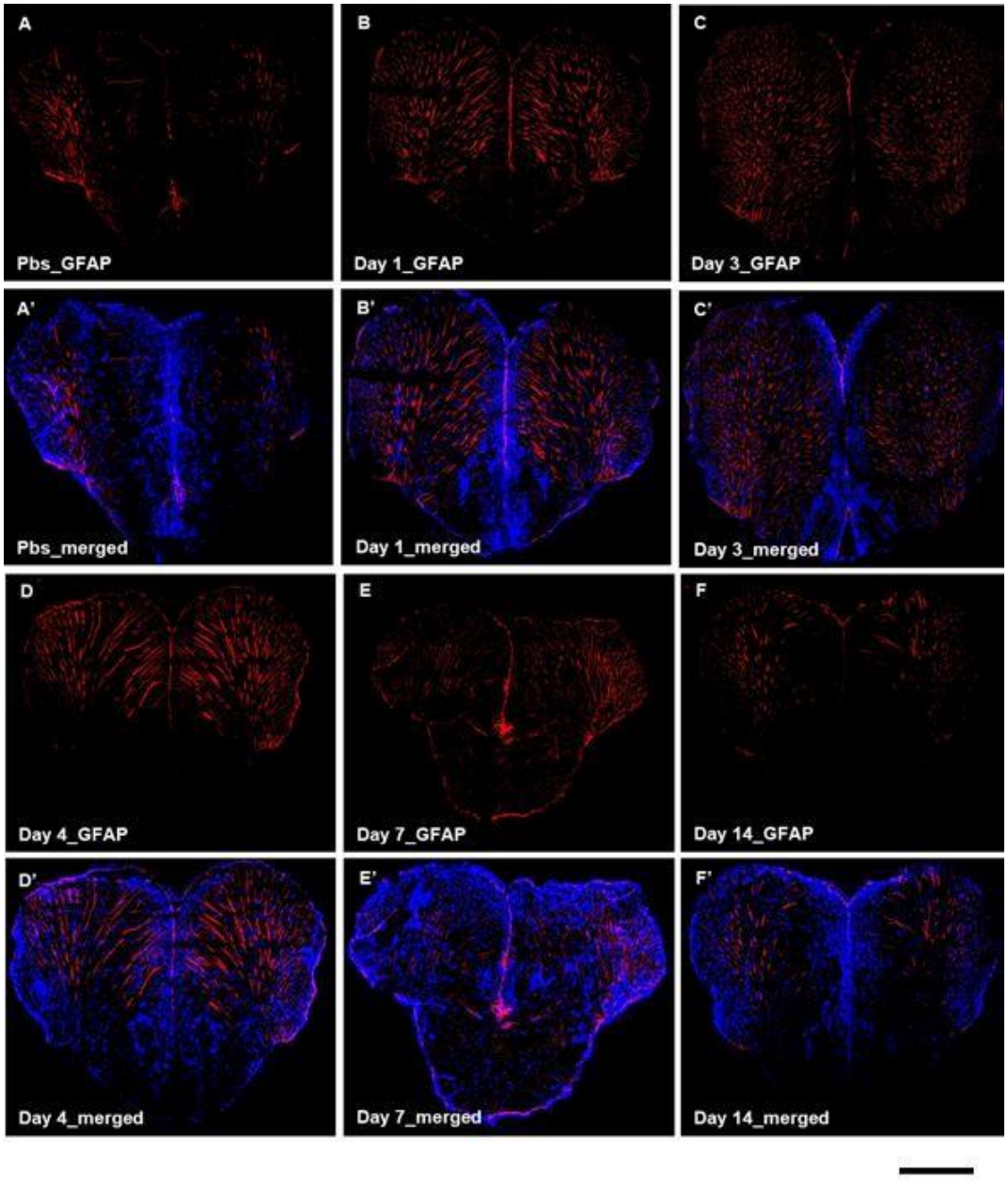

Figure 7: Anti-GFAP immunofluorescence staining (Anti-GFAP immunostaining of brain section obtained from PBS (A), 1dpi (B), 3 dpi (C), 4dpi (D), 7dpi (E), 14dpi (F) A' , B' , C' , D', E', F' represent the DAPI staining. Scale bars 100µm).

In the staining, the GFAP level, which spread in the dorsal telencephalic area from the 1st day, decreased in the ventral and dorsal nucleus of the telencephalic area on the 3rd day. The decreased GFAP level in the ventral telencephalon and Sub-Pallium on the 4th day of the injection was less than the GFAP level observed even in the control group as of the 14th day (Figure 7).

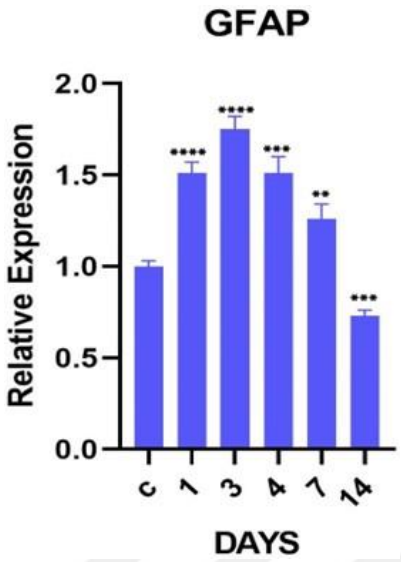

Figure 8: Real-time PCR analysis of mRNAs for GFAP. *rpl13* was used as endogenous control. The relative mRNA level was normalized to the corresponding *rpl13* mRNA expression. qPCR data presented here are means ± SD from triplicate data. Asterisk on individual bars represents a significant difference between the control group and NCP groups. Student's t-test was used to calculate significance *P < 0.05, **P < 0.01, ***P < 0.001 (Student's unpaired t-test). Error bars indicate SEM.

As a result of qPCR performed as the quantification of immunofluorescent images, when the relative expression level of the control group injected with PBS was accepted as 1, the increase in GFAP on the first day reached the 1.5 level and the highest level of 1.75 on the 3rd day. The GFAP level, which decreased after the 3rd day after the injection, decreased to 0.73 on the 14th day, below the control group injected with PBS (Figure 8).

3.1.3 Determination of neuronal inflammation and apoptosis levels in Alzheimer's Disease induced by AB42 toxicity in adult zebrafish brain

It has been known that activated microglia secrete potentially neurotoxic proinflammatory cytokines, and this secretion has an effect on the formation of reactive oxygen and nitrogen species and increases neuronal damage (Wang et al, 2015).

To determine the neuronal inflammation caused by AB42 toxicity and the apoptosis caused by neuronal inflammation, c-caspase-3 staining was performed on brain sections.

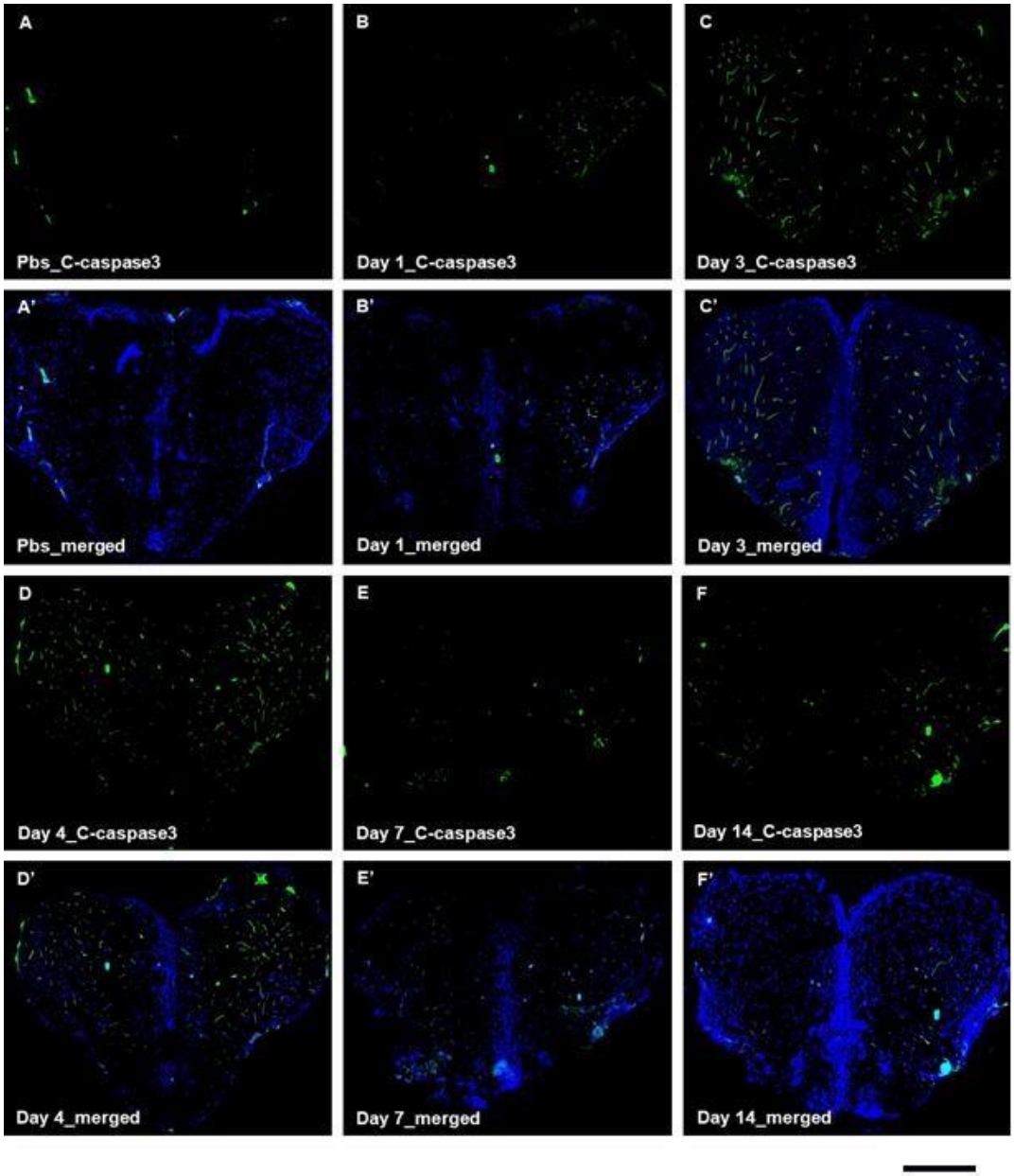

Figure 9: Anti-Cleaved Caspase-3 immunofluorescence staining (Anti-Cleaved Caspase3 immunostaining of brain section obtained from PBS (A), 1dpi (B), 3 dpi (C), 4dpi (D), 7dpi (E), 14dpi (F) A' , B' , C' , D', E', F' represent the DAPI staining).

Cleaved-caspase staining, which showed an increase in the Pallium region the first day after injection, strikingly showed that cell death was widespread in the whole brain on the 3rd and 4th days; on the 7th and 14th days, it decreased close to the control group (Figure 9).

3.1.4 Validation of Neuronal Degradation in Alzheimer's Diseases induced by AB42 toxicity in adult zebrafish brain

HUC/D staining was performed after making sure of the resulting toxicity, to observe the effects of this toxicity on neurons.

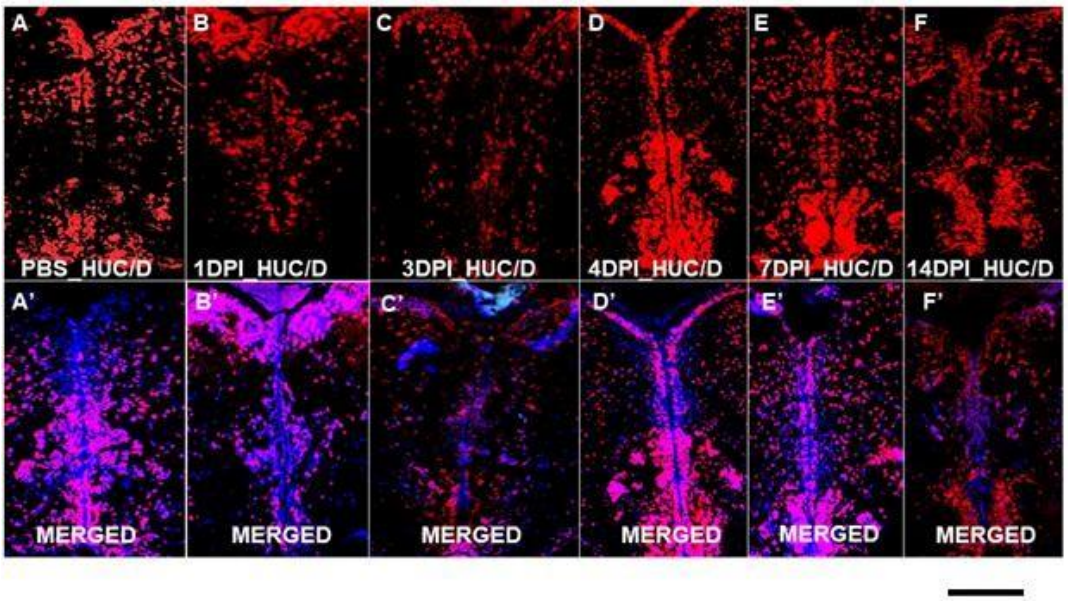

Figure 10: HUC/D immunofluorescence staining (Anti-HUC/D immunostaining of brain section that obtained from PBS (A), 1dpi (B), 3 dpi (C), 4dpi (D), 7dpi (E), 14dpi (F) A' , B' , C' , D', E', F' represent the DAPI staining. Scale bars 100µm).

Since we knew that toxicity was fully formed on day 3 in our previous studies, losses in the dorsal telencephalic area and ventral telencephalic area seen in the HUC/D staining on the 3rd day were evidence of neuronal degeneration. However, we observed that no remarkable change was detected on days 4-7-14dpi, where toxicity caused short-term neuronal losses, but the brain restored this until the 14 days were completed (Figure 10).

Since the immunofluorescent stains are not very distinguishable, the mRNA levels of the HUC and HUD were checked by qPCR to confirm the results.

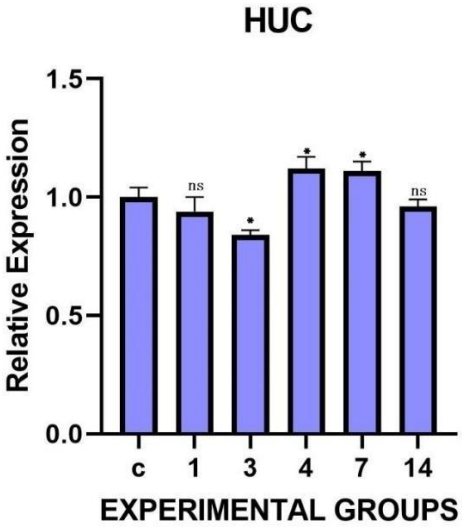

Figure 11. Real-time PCR analysis of mRNAs for HUC. *rpl13* was used as endogenous control. The relative mRNA level was normalized to the corresponding *rpl13* mRNA expression. qPCR data presented here are means ± SD from triplicate data. Asterisk on individual bars represents a significant difference between the control group and NCP groups. Student's t-test was used to calculate significance *P < 0.05, **P < 0.01, ***P < 0.001 (Student's unpaired t-test). Error bars indicate SEM.

According to the HUC qPCR results, although the number of HUC mRNA levels starting on the first day was not statistically significant, the neuronal degeneration on the 3rd day, which was also seen in the immunofluorescent staining, decreased approximately 1.25 times below the control group injected with only PBS. The brain restored itself by increasing the neuronal density and regeneration process from 3 dpi to 14 days and reached almost the same level as the control group at 14 dpi (Figure 11).

3.1.5 Molecular characterization of the regenerative response in an adult zebrafish AD model based on Aß neurotoxicity

After the results, which we determined that the neuronal degeneration process returned to normal towards the 14th day, we performed immunofluorescence staining with anti-phosphobetacatenin antibody for the transcriptional marker phosphobetacatenin to detect the level of the Wnt/β-catenin signaling pathway.

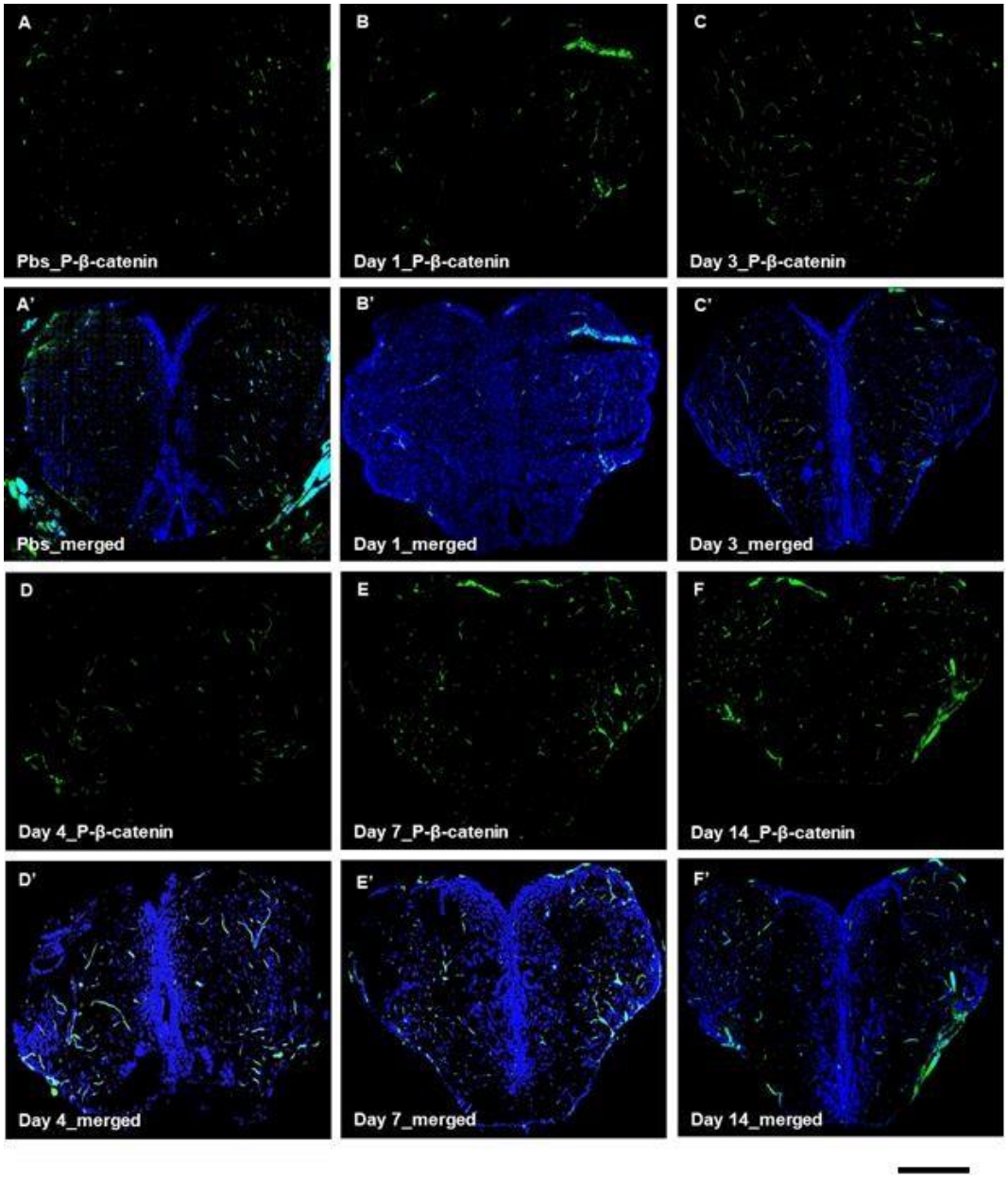

Figure 12: Phospho-β-catenin immunofluorescence staining (Phospho-β-catenin immunostaining of brain section obtained from PBS (A), 1dpi (B), 3 dpi (C), 4dpi (D), 7dpi (E), 14dpi (F) A' , B' , C' , D', E', F' represent the DAPI staining. Scale bars 100µm).

In the staining of the telencephalon tissue, an elevation in the number of cells positive for beta-catenin was revealed from the 1st to the 14th day of toxicity. The high accumulation of amyloid plaques at 7dpi, where the number of β-catenin positive cells is the highest, confirmed the hypothesis of activating the Wnt/β-catenin signaling pathway to clear plaques formed in the brain. Thus, we conclude that Wnt/β-catenin signaling is activated in response to toxicity occurring in the brain (Figure 12).

3.2. Investigation of the role of Wnt/β-catenin signal transduction in AD caused by Aß neurotoxicity and in the formation of regenerative response caused by AD

Wnt/β-catenin signal transduction is one of the most common intracellular signal transduction pathways activated in response to injury to almost all tissues/organs (Ozhan & Weidinger, 2014; 2015).

In studies performed in this thesis, Tcf/Lef has been shown to precisely detect Wnt/β-catenin pathway activity in various cellular contexts to reveal whether Wnt/β-catenin signaling is activated in the process of Aβ42-induced neurotoxicity creating the pathogenesis of AD and the formation of the neuronal regeneration response against it we used the transgenic zebrafish line Tg(6XTCF:d2EGFP) (short for 6XTCF), a reporter of mediated transcription (Shimizu et al., 2012).

3.2.1 Detection of the change of Alzheimer's-related genes by days in 6XTCF transgenic line and imaging of amyloid beta plaques on brain sections

Expression levels of APPA, APPB PSEN1, and PSEN2 genes associated with Alzheimer's were measured by the qPCR method. According to the results, the APPA gene, which was 2 times upregulated in 1dpi, 3dpi, and 4dpi, was observed to be upregulated approximately 1.2 times that of the control with a decrease after the 4th day, but it was not statistically significant. At 14dpi, it was observed to be upregulated about 3 times the control. Similarly, in the APPB gene examined, the APPB gene, which increased 1.5 times that of the control at 1dpi, 4dpi, and 14dpi, had an expression level of 0.5 when the control was accepted as 1 on the 7th day. A critical increase from 7 dpi to 14 dpi was observed in this gene, as in APPA, and the changes according to days in these two genes were found to be consistent.

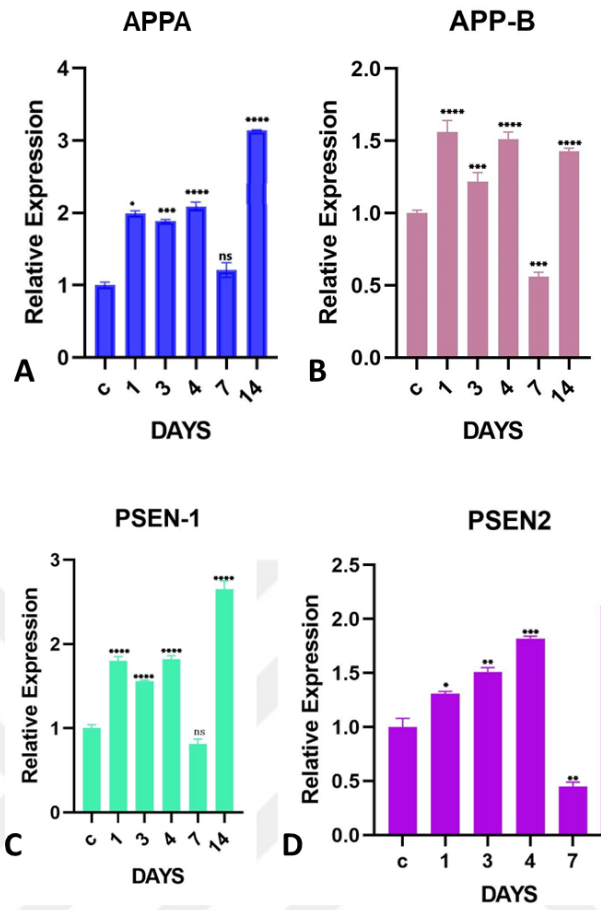

Figure 13: Real-time PCR analysis of mRNAs for APPA, APPB, PSEN1, and PSEN2. *rpl13* was used as endogenous control. The relative mRNA level was normalized to the corresponding *rpl13* mRNA expression. qPCR data presented here are means ± SD from triplicate data. Asterisk on individual bars represents a significant difference between the control group and NCP groups. Student's t-test was used to calculate significance *P < 0.05, **P < 0.01, ***P < 0.001 (Student's unpaired t-test). Error bars indicate SEM.

The model we created triggers amyloid deposition, which is an important process in Alzheimer's Disease. APP genes must be cut by beta-secretase and gamma-secretase to form amyloid beta. Presenilins are subcomponents of gamma-secretase, which is responsible for the cleavage of APP. Accordingly, qPCR was performed on the samples taken at 1dpi,3dpi,4dpi,7, and 14dpi too to examine the changes in the mRNA level of Presenilin genes in the toxicity that was created (Figure 13).

The results showed that; although there were varying levels of increases in the psen1 gene until day 4, a dramatic downregulation occurred on day 7 up to almost half of the control group. From 7dpi to 14dpi, gene expression level reached 2.5 times of expression compared to the control group which is the highest expression level within 14 days. Although there is a gradual increase up to 4dpi in the results of psen2, there has been a dramatic downregulation in 7dpi

similar, it has reached the highest expression level in 14dpi.

Next, we aimed to investigate the effect of expression increases of Alzheimer's-related genes at mRNA levels on the accumulation of amyloid beta plaques, and brains were dissected from fish injected with Aß following the protocols described in Method 2.4 at 1 dpi, 3dpi, 4 dpi, 7 dpi, and 14 dpi, brain sections were taken, and anti-Aβ42 was applied to the sections on the aforementioned days primarily for the occurrence of Aβ42 toxicity immunofluorescent staining was done (Figure 14).

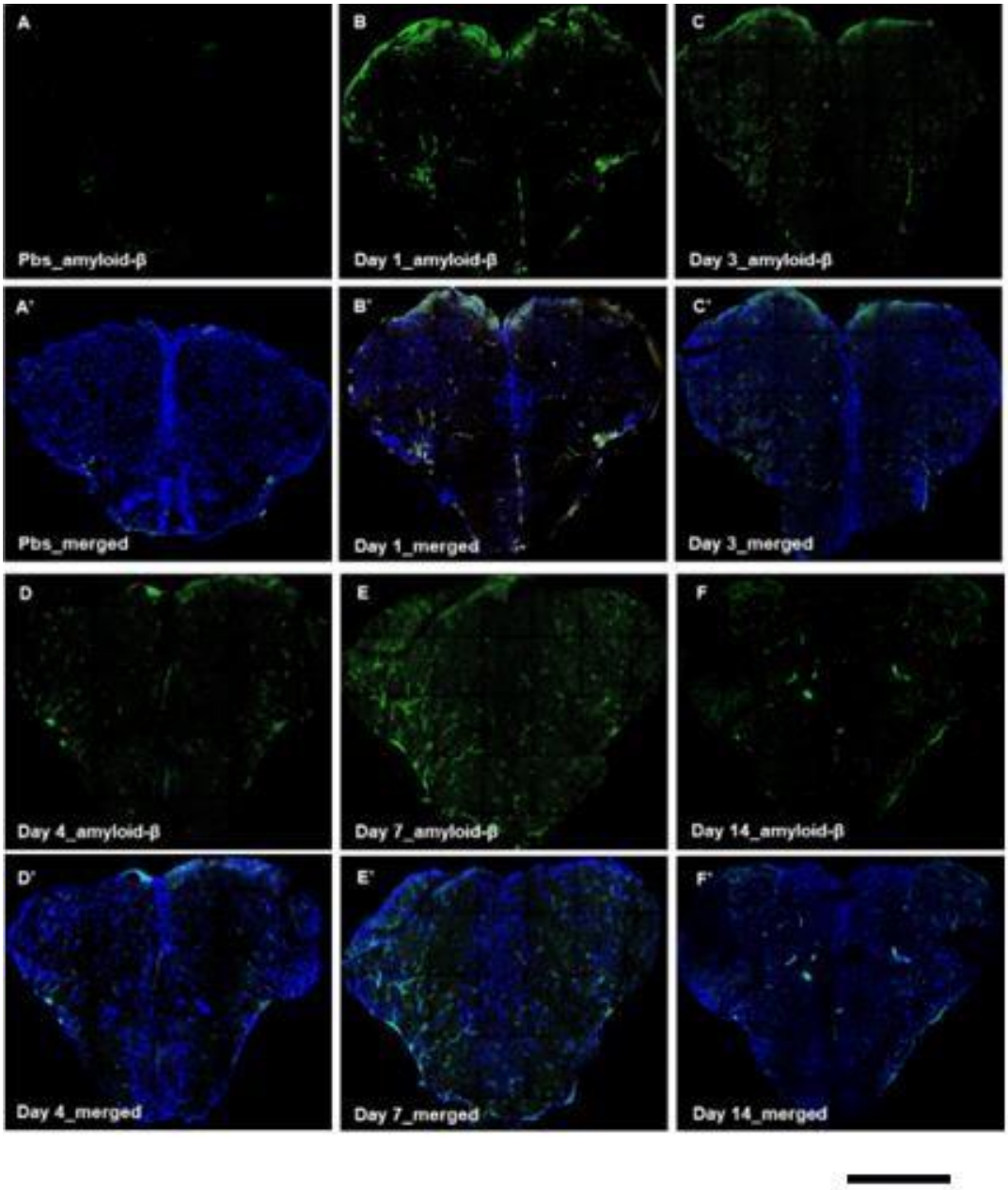

Figure 14: Anti-Aβ42 immunofluorescence staining (Anti-Aβ42 immunostaining of brain section obtained from PBS (A), 1dpi (B), 3 dpi (C), 4dpi (D), 7dpi (E), 14dpi (F) A' , B' , C' , D', E', F' represent the DAPI staining. Scale bars 100µm).

3.2.2 Revealing the mRNA-level activity of Wnt/β-catenin signaling in the pathogenesis of Aβ42 toxicity-induced AD

In the pathogenesis of AH caused by Aβ42 toxicity; to reveal the activity of Wnt/β-catenin signal transduction at the mRNA level in the formation of the dynamic structure of Aβ42 accumulation, the changes in the expressions of the EGFP gene, which is the reporter of Wnt activity in the brain of 6XTCF fish injected with Aß were investigated. Expressions of genes were analyzed by applying RNA isolation, cDNA synthesis, and qPCR protocol at 1 dpi, 4 dpi, 7 dpi, and 14 dpi from telencephalon tissue (Demirci et al., 2020).

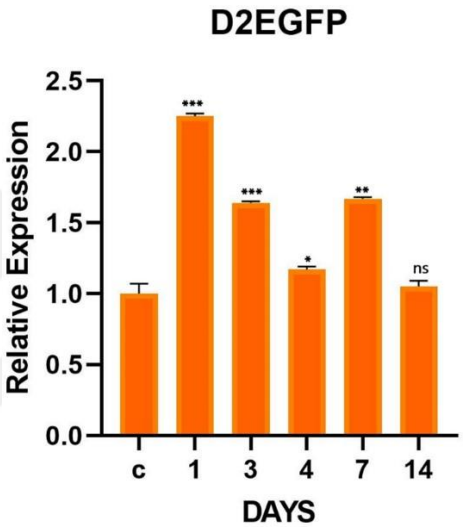

Figure 15: Real-time PCR analysis of mRNAs for D2EGFP. *rpl13* was used as endogenous control. The relative mRNA level was normalized to the corresponding *rpl13* mRNA expression. qPCR data presented here are means ± SD from triplicate data. Asterisk on individual bars represents a significant difference between the control group and NCP groups. Student's t-test was used to calculate significance *P < 0.05, **P < 0.01, ***P < 0.001 (Student's unpaired t-test). Error bars indicate SEM.

In the mRNAs obtained from the telencephalon tissue, on the 1dpi of, a 2-fold upregulation occurred in the EGFP gene, the reporter of the Wnt/β-catenin signaling pathway, and it was statistically significant. Wnt signal transduction, which showed a gradual decrease from 1dpi to 4dpi, was observed to increase again by 1.5 times on the 7th day and was at the same level as the control group injected with PBS on the 14th day (Figure 15).

To determine the Wnt/β-catenin signaling activity, immunofluorescent staining was performed on the sections with anti-EGFP and anti-phospho-β-Catenin (Ser675) antibodies, which are markers of β-Catenin transcriptional activity.

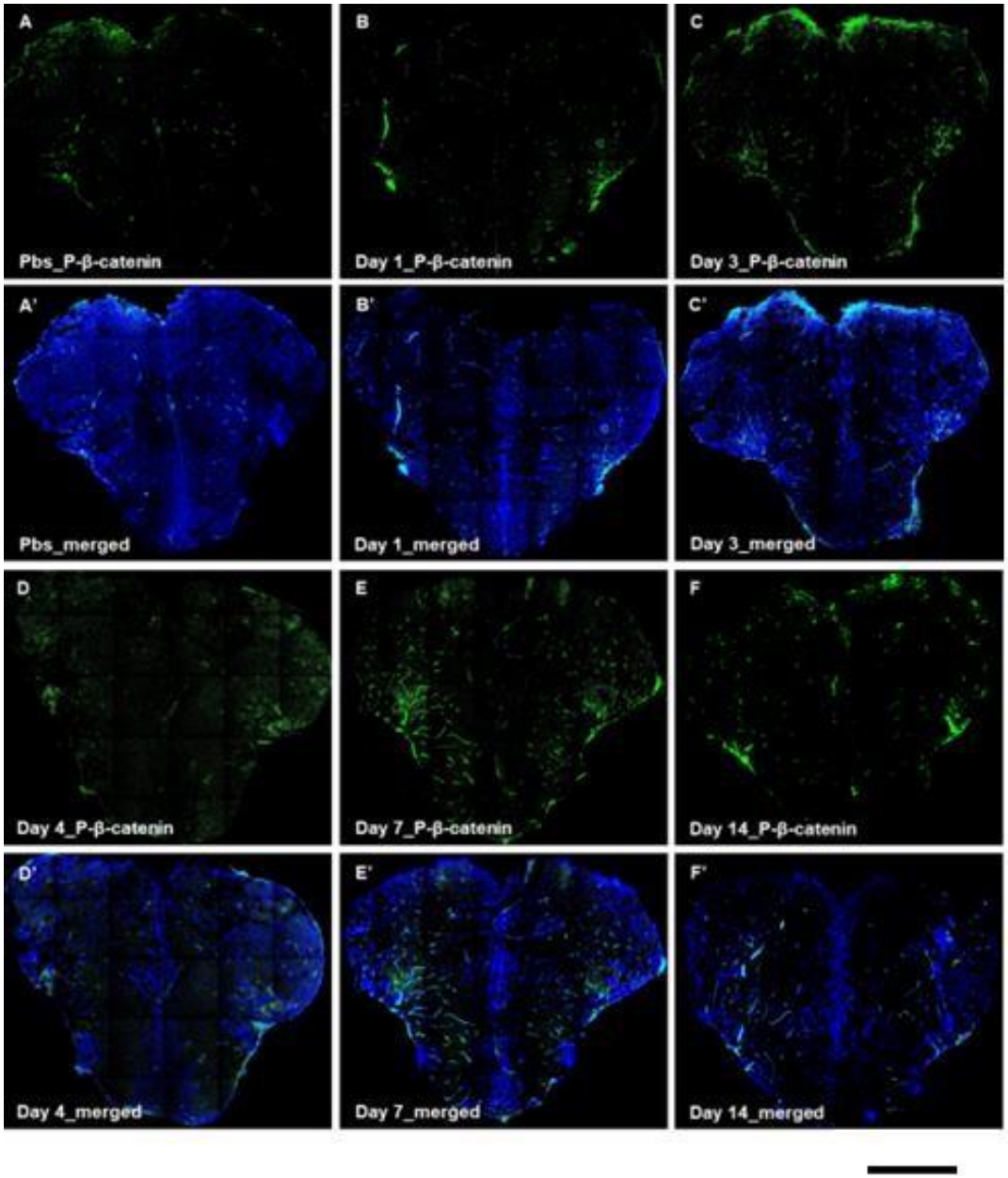

Figure 16: Anti-phospho-β-Catenin immunofluorescence staining (anti-phospho-β-Catenin immunostaining of brain section obtained from PBS (A), 1dpi (B), 3 dpi (C), 4dpi (D), 7dpi (E), 14dpi (F) A' , B' , C' , D', E', F' represent the DAPI staining. Scale bars 100µm).

Wnt/β-catenin signaling pathway becomes activated in the regenerating zebrafish telencephalon at the traumatic brain injury and early wound healing stage and promotes tissue-wide regeneration. The brain sections taken from the telencephalon region revealed elevation of phosphobetacatenin on the 1dpi and 7 dpi. This elevation was also reflected in the number of phosphobetacatenin-positive cells. Signaling activation of Wnt/β-catenin was observed to be predominantly in places where amyloid plaques accumulated (Figure 16).

For the detection of signal transduction, it was observed that the increase in 1dpi and 7dpi in

the Anti-EGFP immunofluorescent painting with the phosphobetacatenin was also reflected in anti-EGFP stainings.

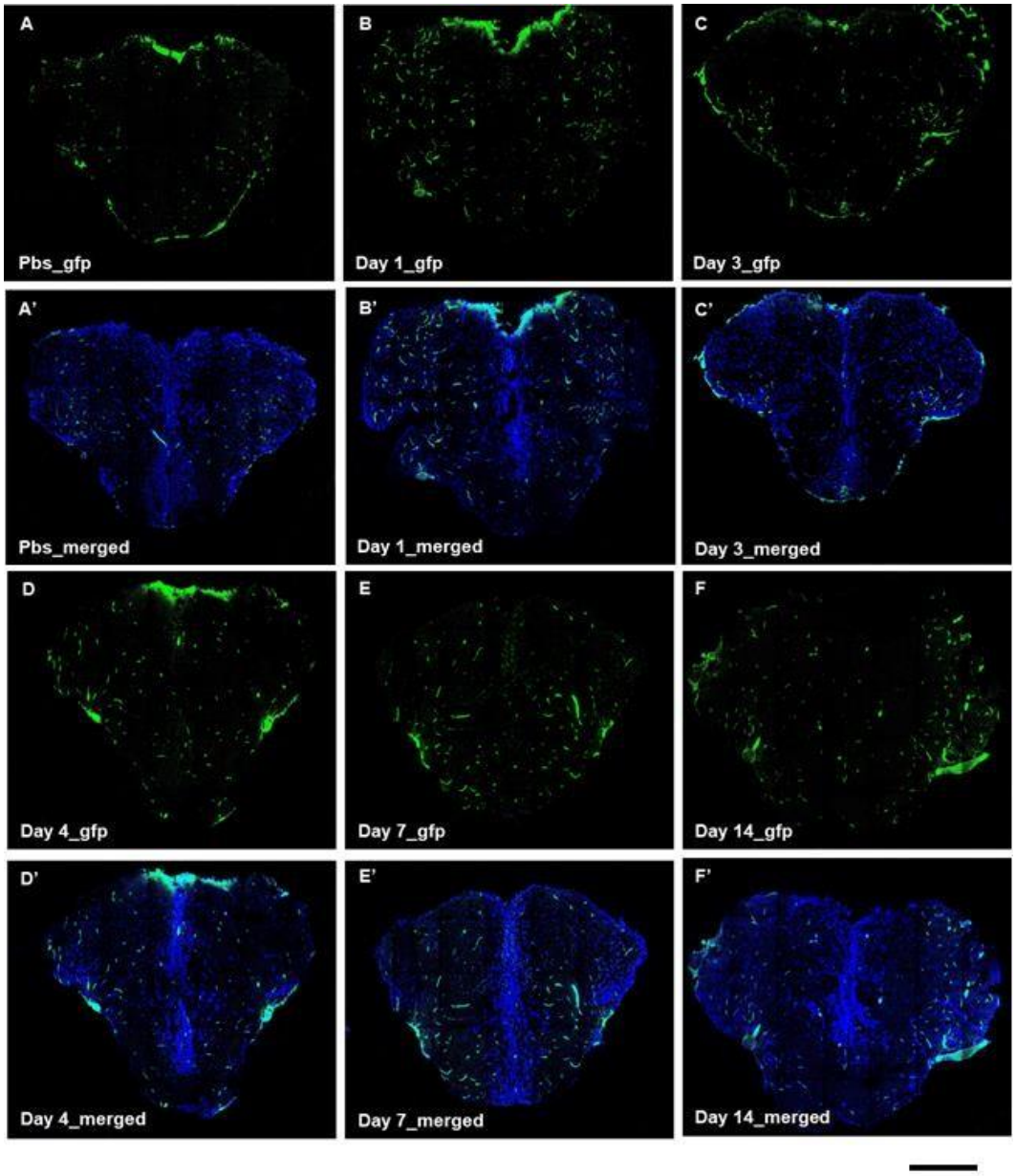

Figure 17: Anti-GFP immunofluorescence staining (Anti-GFP immunostaining of brain section obtained from PBS (A), 1dpi (B), 3 dpi (C), 4dpi (D), 7dpi (E), 14dpi (F) A' , B' , C' , D', E', F' represent the DAPI staining. Scale bars 100µm).

In addition, amyloid beta accumulation was found to be at the lowest level on 1dpi and 7dpi compared to the control group. As well as genes related to Alzheimer's at the lowest levels when WNT/Beta Catenin is the highest activity. Therefore, next, we aimed to test whether WNT activity is necessary for various cellular events in Aβ42 -induced neuronal degeneration and regeneration processes (Figure 17).

Moreover, we aimed to reveal the characteristics of cell types that are positive for Wnt/β-catenin activity, and immunofluorescence staining was performed with the glial marker S100, and qPCR analysis was performed for NeuroD1 GFAP, HuC, and HuD, which are neuronal and glial markers (Figure 18).

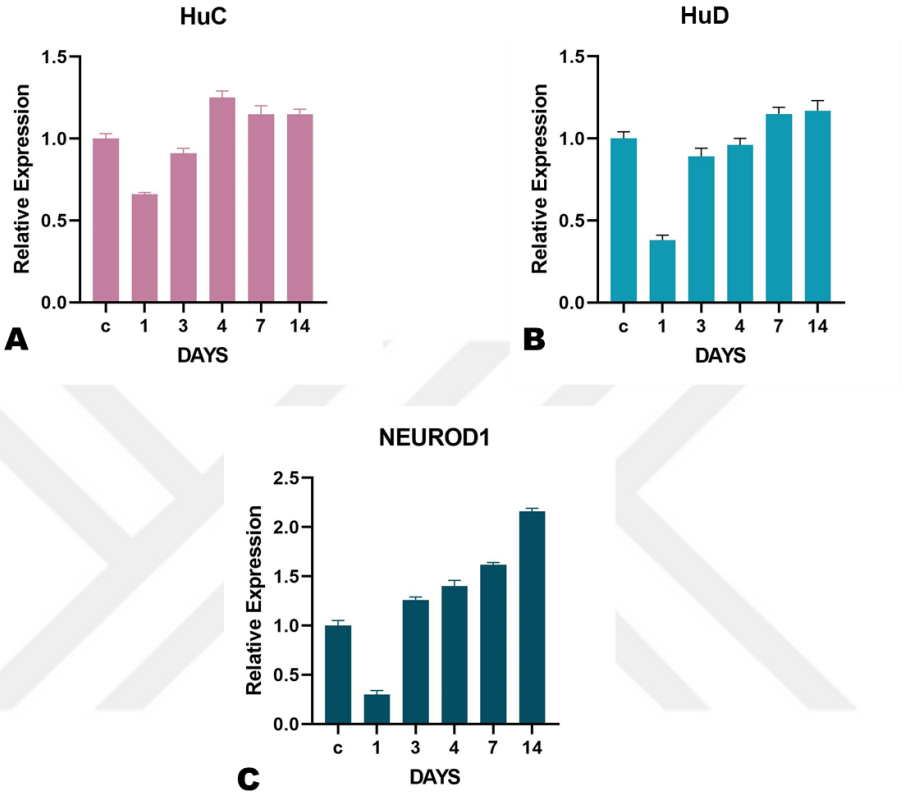

Figure 18: Real-time PCR analysis of mRNAs for HuC, HuD, and NEUROD1. *rpl13* was used as endogenous control. The relative mRNA level was normalized to the corresponding *rpl13* mRNA expression. qPCR data presented here are means ± SD from triplicate data. Asterisk on individual bars represents a significant difference between the control group and NCP groups. Student's t-test was used to calculate significance *P < 0.05, **P < 0.01, ***P < 0.001 (Student's unpaired t-test). Error bars indicate SEM.

A dramatic decrease was observed in neurod1-HuC-HuD expression on the first day of injection, and it was observed that neuron loss was short-term in toxicity, which gradually increased expression at 3,4,7,14 dpi in all three neuron markers, and zebrafish compensated for this loss in the long term.

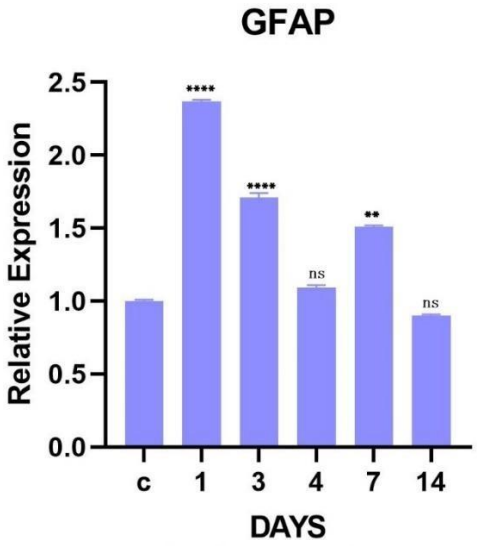

Figure 19: Real-time PCR analysis of mRNAs for GFAP. *rpl13* was used as endogenous control. The relative mRNA level was normalized to the corresponding *rpl13* mRNA expression. qPCR data presented here are means ± SD from triplicate data. Asterisk on individual bars represents a significant difference between the control group and NCP groups. Student's t-test was used to calculate significance *P < 0.05, **P < 0.01, ***P < 0.001 (Student's unpaired t-test). Error bars indicate SEM.

In glial cell activation, the upregulation at 1dpi and 7dpi and the gradual decrease in 3, 4, and 14 dpi are similar to d2EGFP and phosphobetacatenin. By looking at these, it can be said that the cells positive for phosphobetacatenin are glial cells. To confirm these results, s100 staining was performed to observe radial glial cells, which are an indicator of the regeneration response in zebrafish, in brain sections taken.

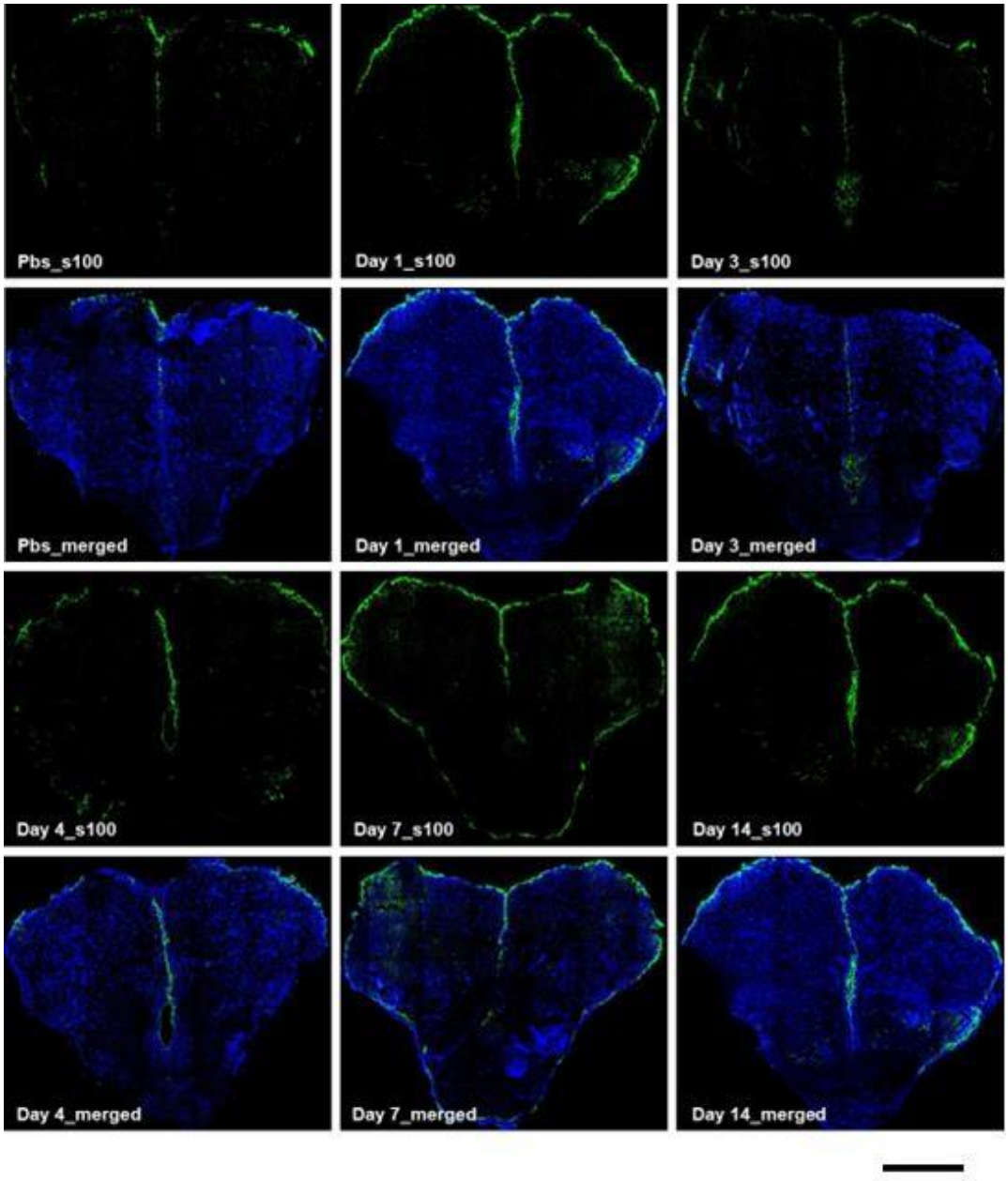

Figure 20: Anti-S100 immunofluorescence staining (Anti-S100 immunostaining of brain section obtained from PBS (A), 1dpi (B), 3 dpi (C), 4dpi (D), 7dpi (E), 14dpi (F) A' , B' , C' , D', E', F' represent the DAPI staining. Scale bars 100µm).

The extinction observed up to Day 4 in activation at 1dpi and reactivation observed at 7dpi overlap with the above qPCR results. It also shows that the regeneration that occurs is concentrated in glial cells (Figure 20).

3.3. Revealing the relationship between Wnt/β-catenin signaling and the pathogenesis of AD

3.3.1 Creation of Experimental Groups

According to the results observed in 3.2.2 the days with high regenerative response were determined as 1dpi and 7dpi. Afterward, we aimed to inhibit WNT activity with IWR-1 drug for 1dpi and 7dpi after Aß injection in the 6XTCF transgenic line.

In the experiments we carried out for 1dpi, we placed the fish 24 hours before the injection in the system water to which we added 10µM DMSO in order to provide the negative control conditions. At the end of 24 hours, the fish were reintroduced into DMSO immediately after PBS was injected with the CVMI method. Transgenic fish that spent 24 hours in DMSO after injection were dissected (Figure 21).

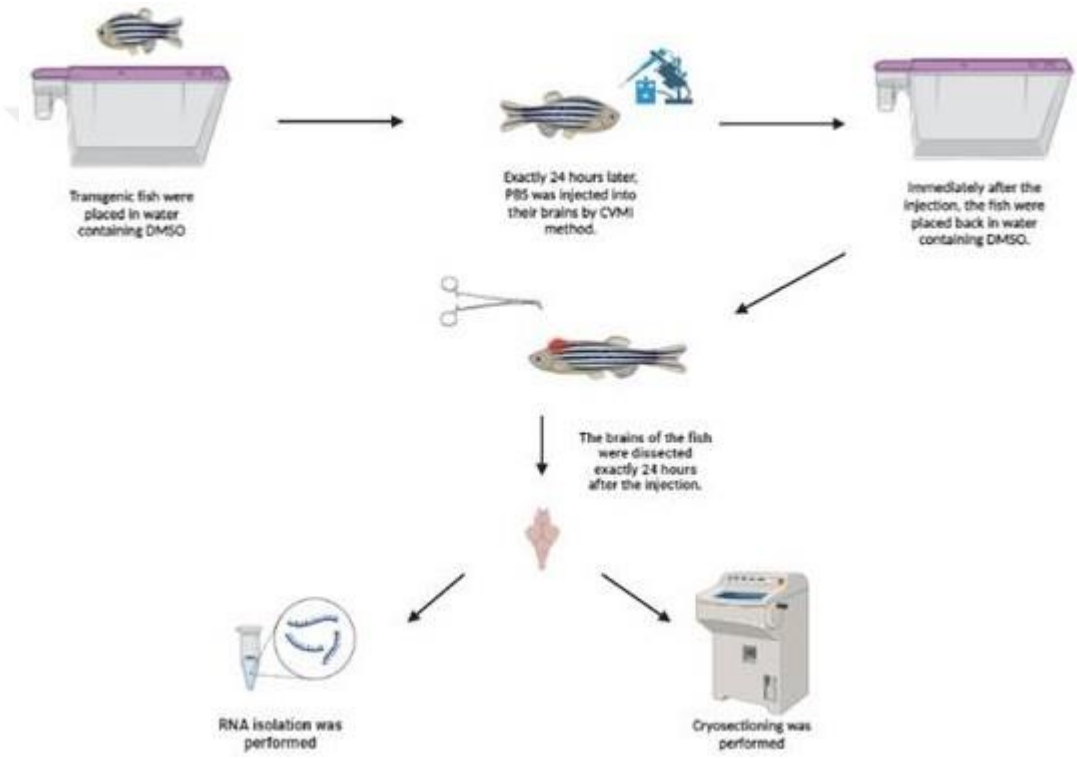

Figure 21: Creation of Negative Control Group for IWR-1 treatment on 1dpi. The figure was generated in BioRender.com.

We placed fish 24 hours prior to injection in system water to which we added 10µM DMSO to ensure positive control conditions for 1dpi. At the end of 24 hours, the fish were reintroduced into DMSO immediately after Aß was injected with the CVMI method. Transgenic fish that spent 24 hours in DMSO after injection were dissected (Figure 22).

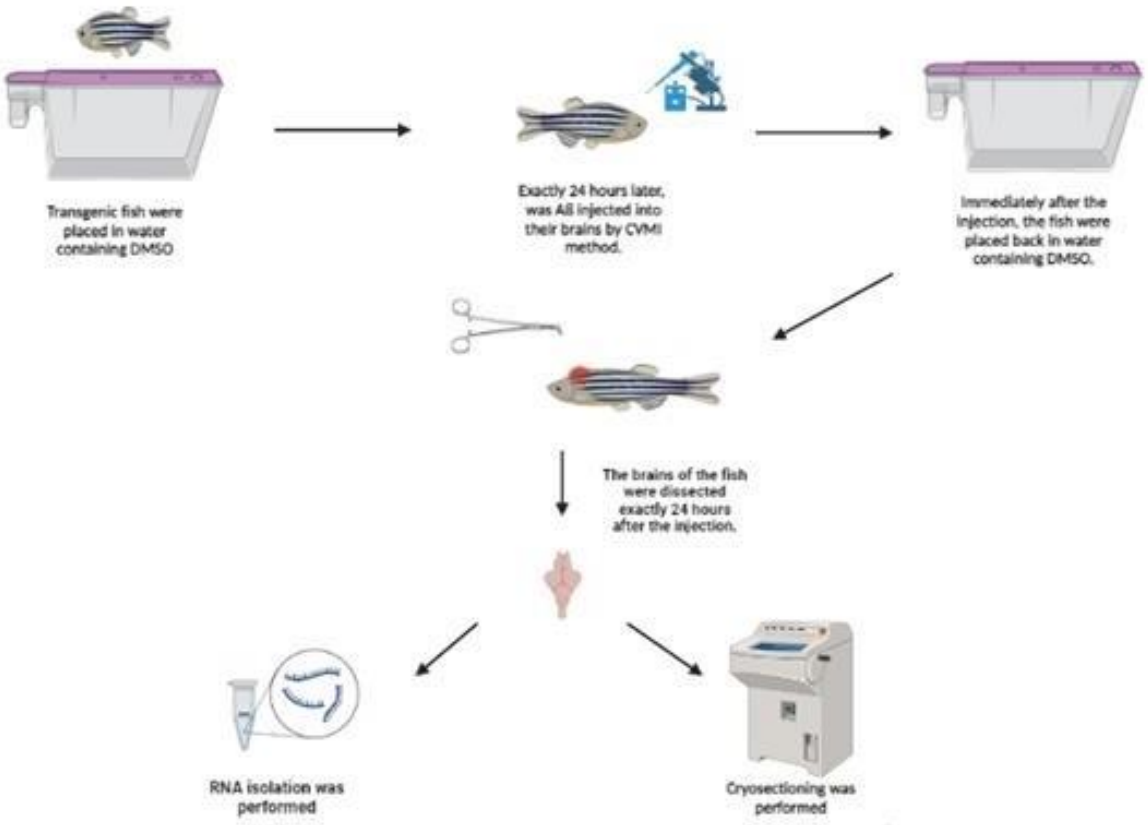

Figure 22: Creation of Positive Control Group for IWR-1 treatment on 1dpi. The figure was generated in BioRender.com.

For the IWR-1 treatment group; The 6XTCF fish, which were added to the system water containing 10µM IWR-1 drug 24 hours before the injection, were taken back to the system water containing IWR-1 immediately after the injection. They were dissected 24 hours after injection (Figure 23).

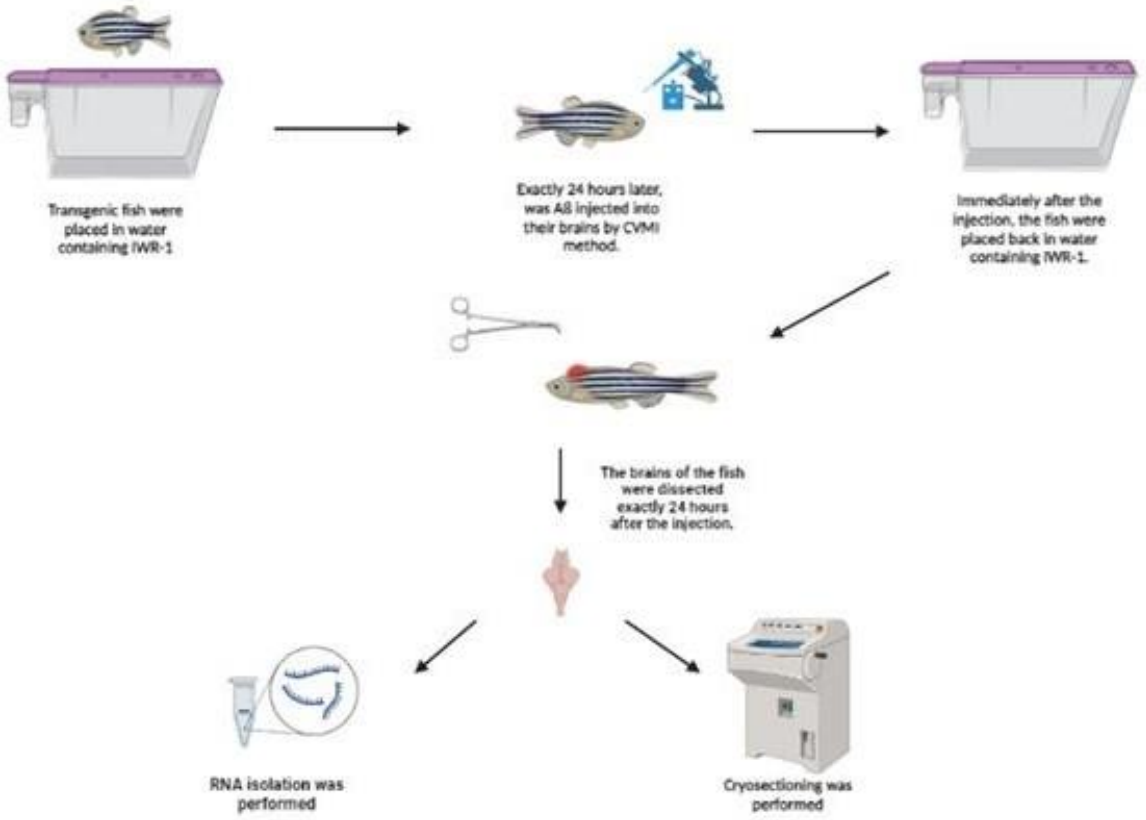

Figure 23: Creation of IWR-1 treatment on 1dpi. The figure was generated in BioRender.com.

In order for the WNT response inhibitor treatment to be performed at 7dpi to be successful, the groups of fish injected with PBS Aß and Aß, respectively, were kept in normal system water until the 4th day, and after 4dpi, they were placed in system water containing 10µM DMSO, DMSO, and IWR-1, respectively. Up to 7dpi drugs were renewed daily and at 7dpi fish were dissected (Figure 24).

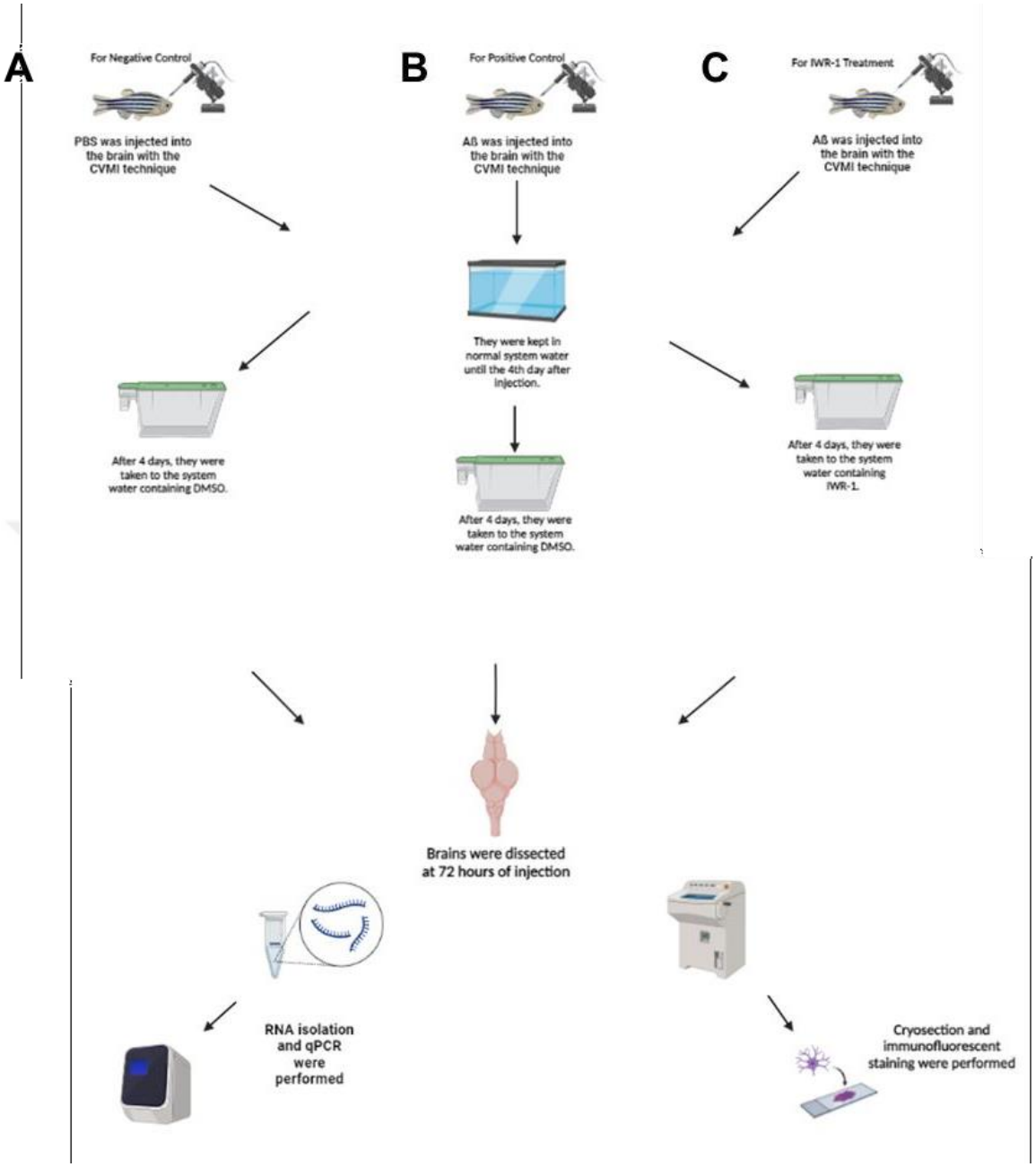

Figure 24: Creation of Experimental Group for IWR-1 treatment on 7dpi. The figure was generated in BioRender.com.

3.3.2 Validation of Aß toxicity in Positive Control Groups

In RNA samples obtained from telencephalon tissue, the expression levels of AD-related genes, which are APPA, APPB, PSEN1, PSEN2, and BACE were determined, and a comparison was made with the days when the expression of these genes was upregulated (Figure 25).

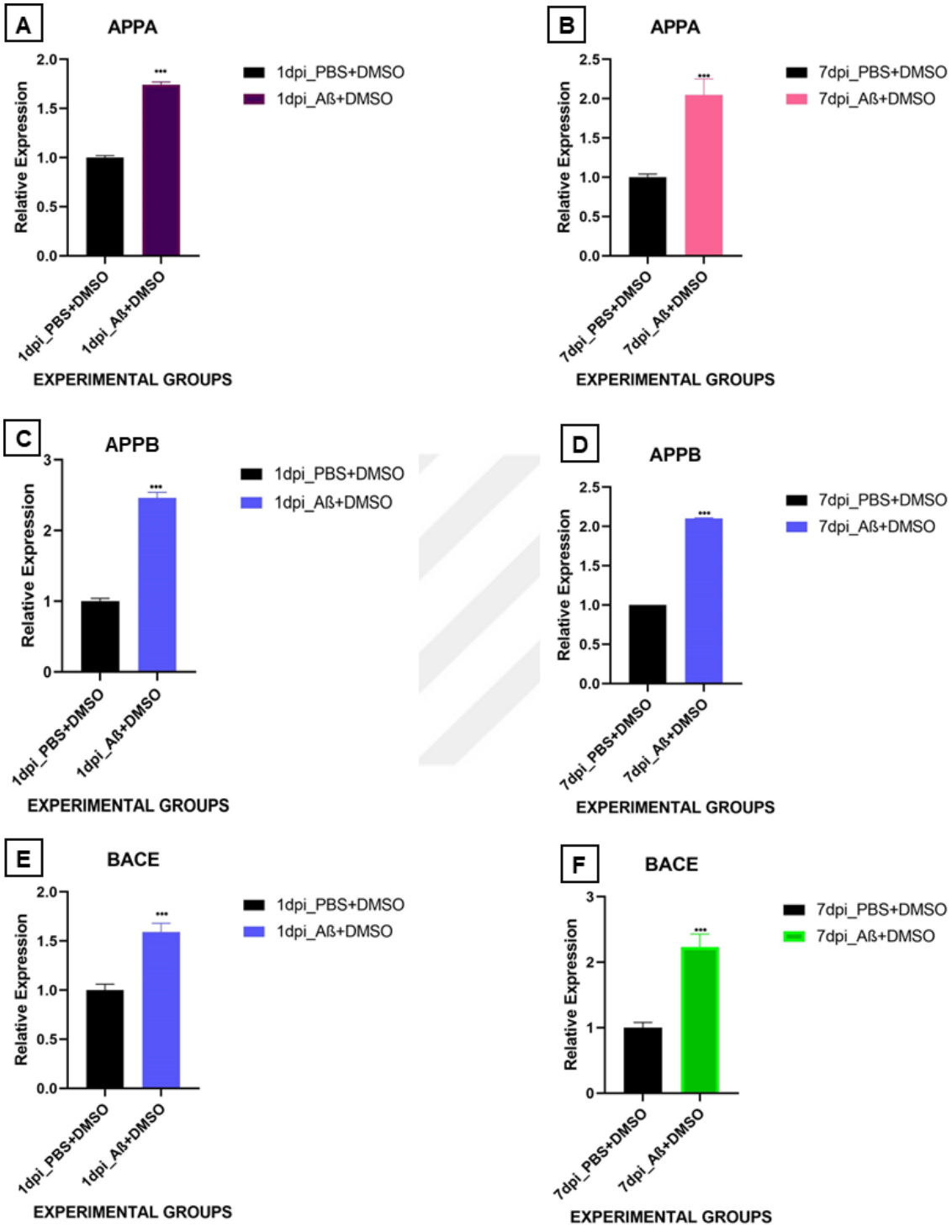

Figure 25: Real-time PCR analysis of mRNAs for APPA, APPB, BACE. *rpl13* was used as endogenous control. The relative mRNA level was normalized to the corresponding *rpl13* mRNA expression. qPCR data presented here are means ± SD from triplicate data. Asterisk on individual bars represents a significant difference between the control group and NCP groups. Student's t-test was used to calculate significance *P < 0.05, **P < 0.01, ***P < 0.001 (Student's unpaired t-test). Error bars indicate SEM.

When the expression levels of APPA, APPB, and BACE were examined, compared to the negative control group injected with only PBS on 1dpi and 7dpi; upregulation in the range of 1.5-2.5 fold was detected in the Aß injected groups, and all of the results were statistically significant (Figure 26).

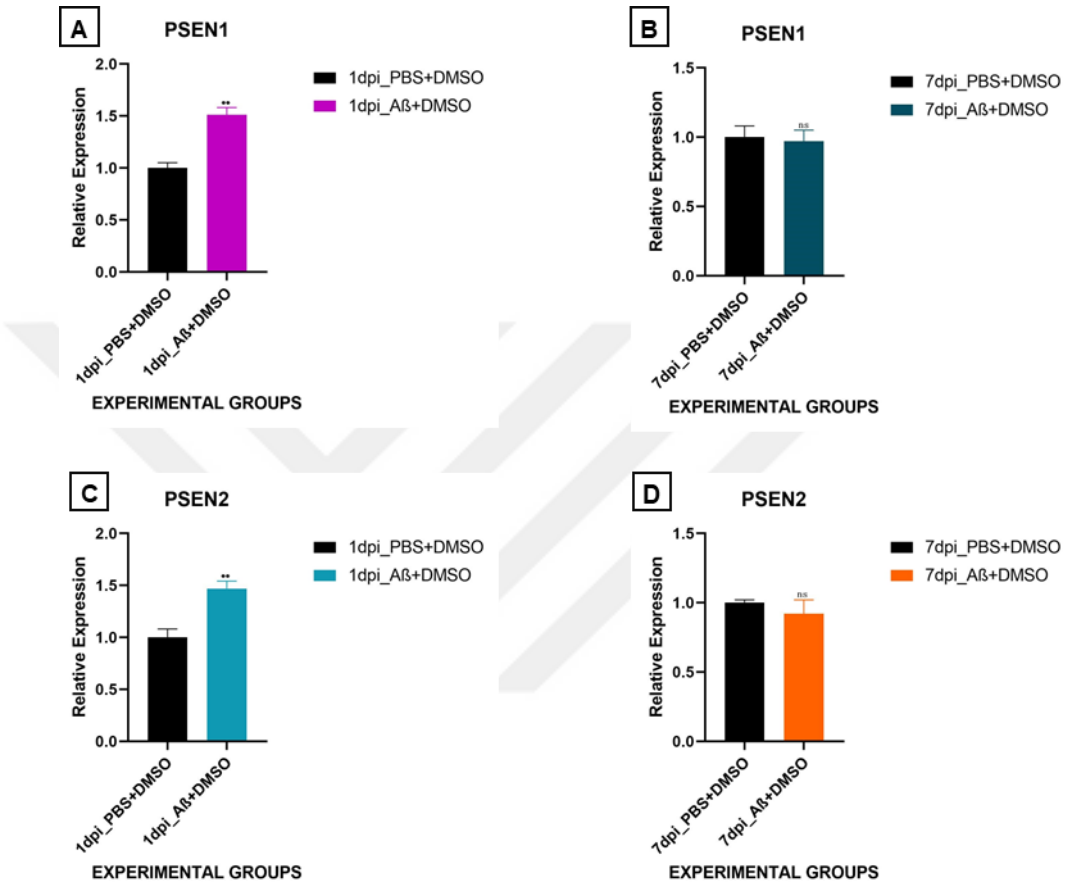

Figure 26: Real-time PCR analysis of mRNAs for PSEN1, and PSEN2. *rpl13* was used as endogenous control. The relative mRNA level was normalized to the corresponding *rpl13* mRNA expression. qPCR data presented here are means ± SD from triplicate data. Asterisk on individual bars represents a significant difference between the control group and NCP groups. Student's t-test was used to calculate significance *P < 0.05, **P < 0.01, ***P < 0.001 (Student's unpaired t-test). Error bars indicate SEM.

When we compare to PSEN1 and PSEN2 genes with the 1dpi_PBS (negative control) group, although there was an elevation in PSEN1 and PSEN2 on 1dpi and it was statistically significant, the same results were not obtained at the gene expression levels measured after 7dpi. A slightly downward change seen at both gene levels was not statistically significant (Figure 27).

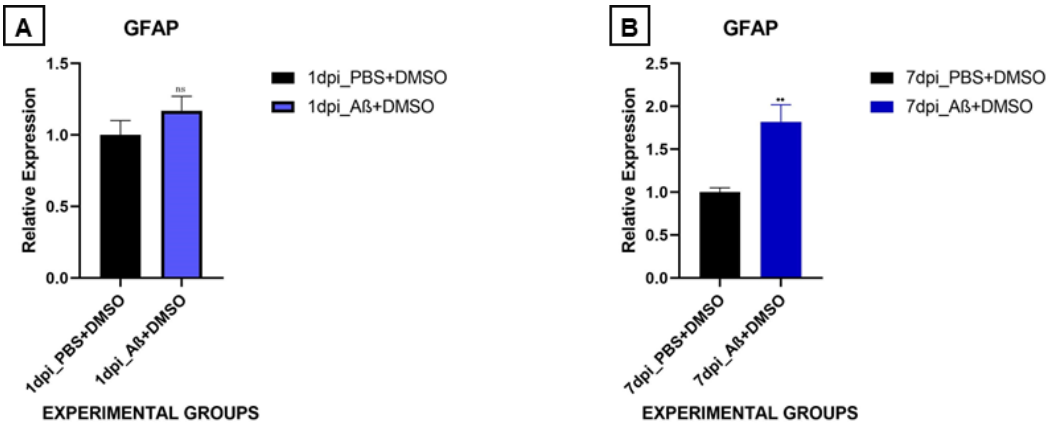

Figure 27: Real-time PCR analysis of mRNAs for GFAP. *rpl13* was used as endogenous control. The relative mRNA level was normalized to the corresponding *rpl13* mRNA expression. qPCR data presented here are means ± SD from triplicate data. Asterisk on individual bars represents a significant difference between the control group and NCP groups. Student's t-test was used to calculate significance *P < 0.05, **P < 0.01, ***P < 0.001 (Student's unpaired t-test). Error bars indicate SEM.

GFAP gene expression levels, which we checked to see the Glial Cell Activation after Aß toxicity and to ensure the formation of toxicity, were higher than the control group in both 1dpi and 7dpi days, and significant, as we expected.

The final stage of validation was to check the regenerative response of 6XTCFs to Aβ42 toxicity and to see if it was consistent with the Result 3.2.2. According to our results, the d2EGFP gene, which is the reporter of the regenerative response, was activated on both days and was observed with an increase of approximately 1.5 times in the group injected with Aß on the 1dpi and 2-fold on 7dpi compared to the negative control group. Once again, it was assured that the toxicity had been successfully created (Figure 28).

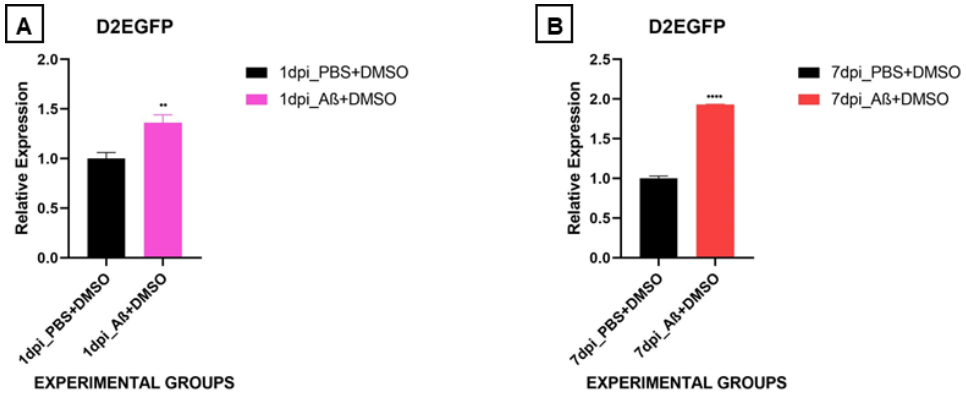

Figure 28: Real-time PCR analysis of mRNAs for D2EGFP. *rpl13* was used as endogenous control. Relative mRNA level was normalized to the corresponding *rpl13* mRNA expression.

qPCR data presented here are means ± SD from triplicate data. Asterisk on individual bars represents a significant difference between the control group and NCP groups. Student's t-test was used to calculate significance *P < 0.05, **P < 0.01, ***P < 0.001 (Student's unpaired t-test). Error bars indicate SEM.

3.3.3 Ensuring Inhibition of Wnt/β-catenin signal transduction by IWR-1 treatment and its Effects on Alzheimer's Disease

A decrease in the regenerative response was expected in transgenic zebrafish treated with IWR-1. First of all, d2EGFP gene expression levels were analyzed in the 1dpi and 7dpi experimental groups created to control this.

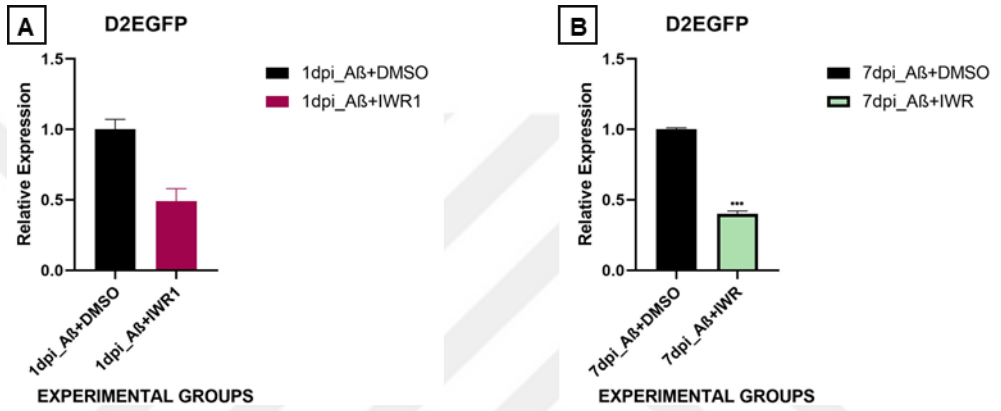

Figure 29: Real-time PCR analysis of mRNAs for D2EGFP. *rpl13* was used as endogenous control. The relative mRNA level was normalized to the corresponding *rpl13* mRNA expression. qPCR data presented here are means ± SD from triplicate data. Asterisk on individual bars represents a significant difference between the control group and NCP groups. Student's t-test was used to calculate significance *P < 0.05, **P < 0.01, ***P < 0.001 (Student's unpaired t-test). Error bars indicate SEM.

In both experimental groups, the expression level of the regenerative response reporter gene decreased by 50% and 52%, respectively, statistically significant as well.

After the IWR treatment was found to be successful, the main question was how to respond to Alzheimer's-related genes due to the low regenerative response that occurred, and the expression levels of Alzheimer's-related genes were controlled separately at 1dpi and 7dpi (Figure 29).

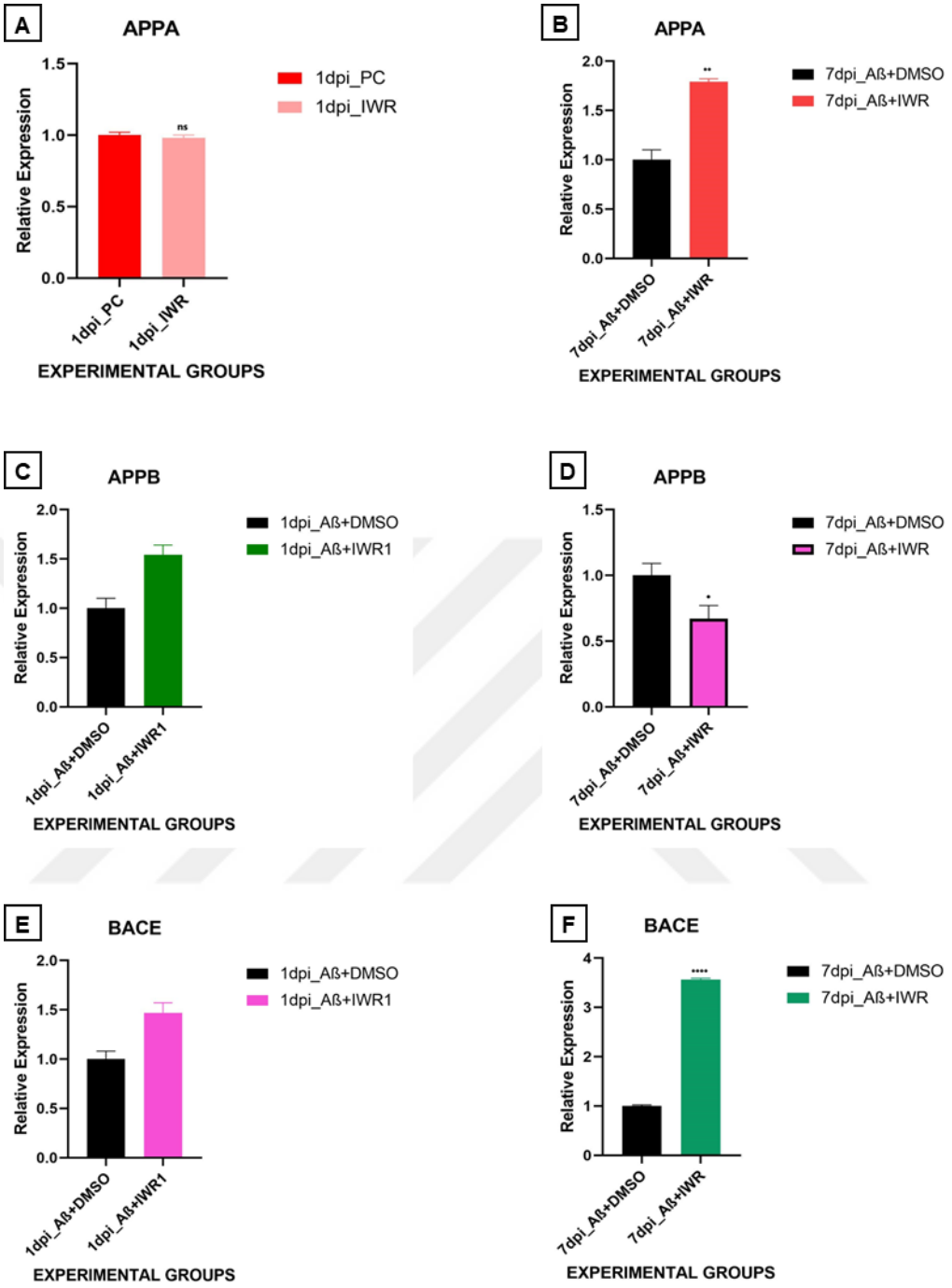

Figure 30: Real-time PCR analysis of mRNAs for APPA, APPB, BACE. *rpl13* was used as endogenous control. The relative mRNA level was normalized to the corresponding *rpl13* mRNA expression. qPCR data presented here are means ± SD from triplicate data. Asterisk on individual bars represents a significant difference between the control group and NCP groups. Student's t-test was used to calculate significance *P < 0.05, **P < 0.01, ***P < 0.001 (Student's unpaired t-test). Error bars indicate SEM.

Although it was observed that the IWR-1 group formed at 1 dpi did not cause any change in the expression level of the APPA gene, the upstream change of APPB and BACE genes in the same

experimental group was quite remarkable. In the same genes analyzed at 7 dpi, the upward increase in APPA and BACE gene expression levels was observed, on the contrary downwards for the APPB gene (Figure 30).

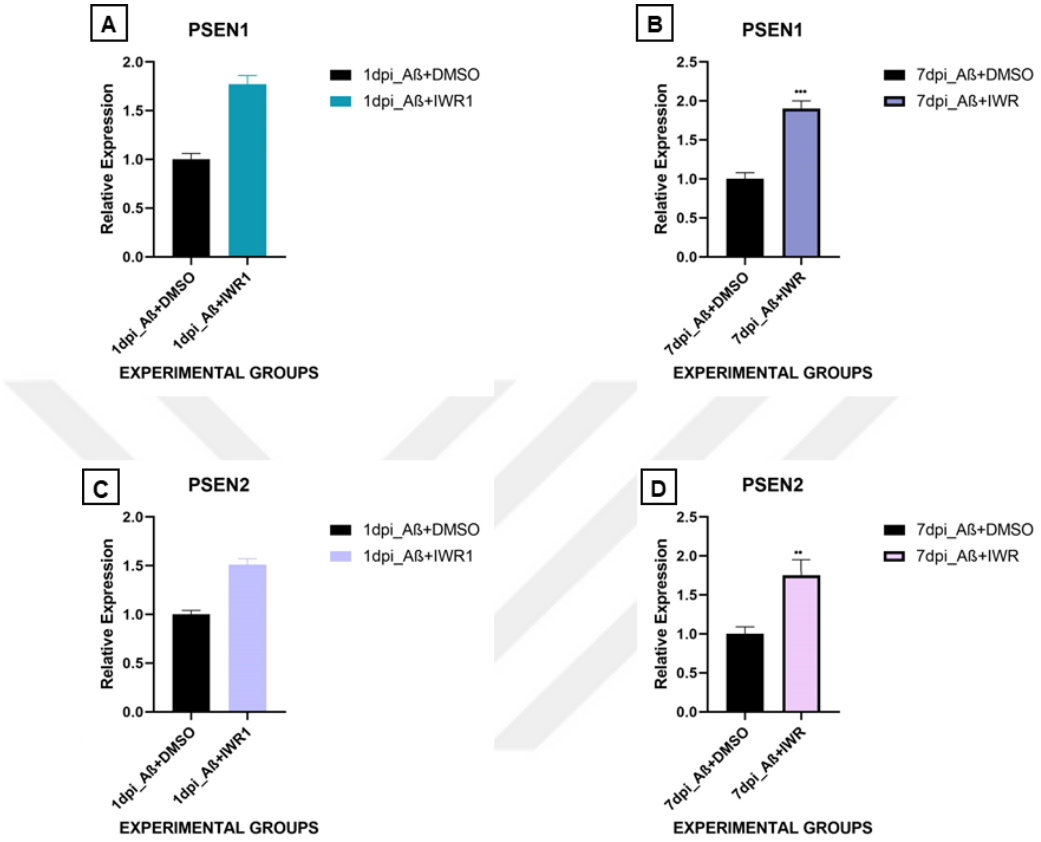

Figure 31: Real-time PCR analysis of mRNAs for PSEN1, and PSEN2. *rpl13* was used as endogenous control. The relative mRNA level was normalized to the corresponding *rpl13* mRNA expression. qPCR data presented here are means ± SD from triplicate data. Asterisk on individual bars represents a significant difference between the control group and NCP groups. Student's t-test was used to calculate significance *P < 0.05, **P < 0.01, ***P < 0.001 (Student's unpaired t-test). Error bars indicate SEM.

In the created model, gene expression levels of PSEN1 and PSEN2 genes, which are also associated with Alzheimer's but mostly increased in Familial Alzheimer's Disease, were controlled and an upward change in both experimental groups was observed after Wnt/β-catenin inhibition was applied. Contrary to what is known, the Wnt/β-catenin pathway was thought to play a more role in Alzheimer's disease, and anti-Aβ42 immunofluorescence staining was applied to the brain sections taken in order to observe the change in the amyloid plaque deposits formed in Alzheimer's disease in the groups in which Wnt inhibition was applied (Figure 31).

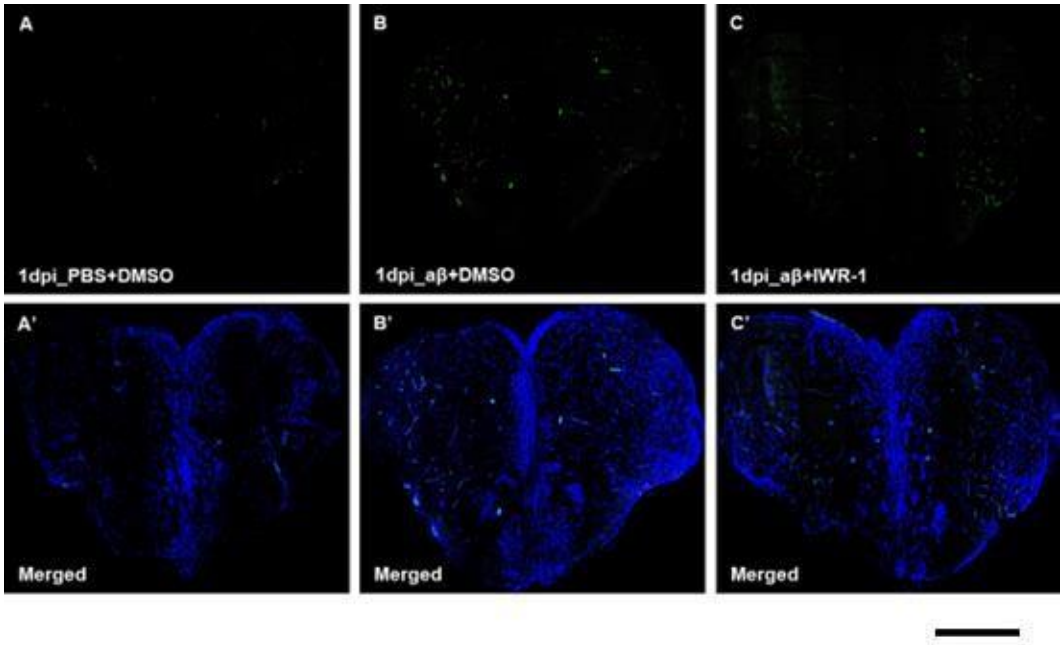

Figure 32: Anti-Aβ42 immunofluorescence staining of 1dpi (Anti-Aβ42 immunostaining of brain section obtained from 1dpi_PBS+DMSO (A), 1dpi_ Aβ+DMSO (B), 1dpi_ Aβ+IWR-1 (C), A' , B' , C' represent the DAPI staining. Scale bars 100µm).

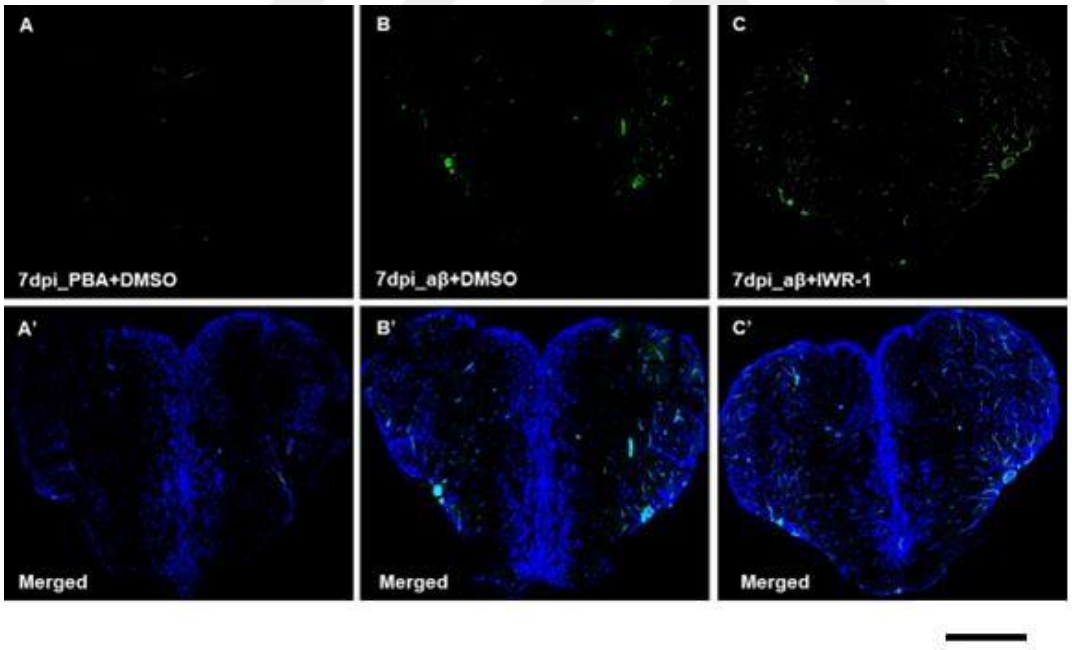

Figure 33: Anti-Aβ42 immunofluorescence staining of 7dpi (Anti-Aβ42 immunostaining of brain section obtained from 7dpi_PBS+DMSO (A), 7dpi_ Aβ+DMSO (B), 7dpi_ Aβ+IWR-1 (C), A' , B' , C' represent the DAPI staining).

The difference between the only-PBS injected group and the Aβ-injected group, seen at 1dpi, allows us to be certain of the toxicity, while the amyloid plaques accumulating between the cells were observed to increase strictly in the IWR-1 treatment-treated groups. According to

these results, no different results were observed in the 7dpi group that was controlled (Figure 32, 33).

Although there was a plaque accumulation in the periventricular area in general in the IWR-1 applied groups, an increase was observed covering the brain tissue in general. It was understood from previous results that a regeneration process started after activation in the glial cells with the increase in the proliferation markers in the brains of zebrafish. In order to control these responses, PCNA and S100 immunofluorescence staining was performed on brain tissues.

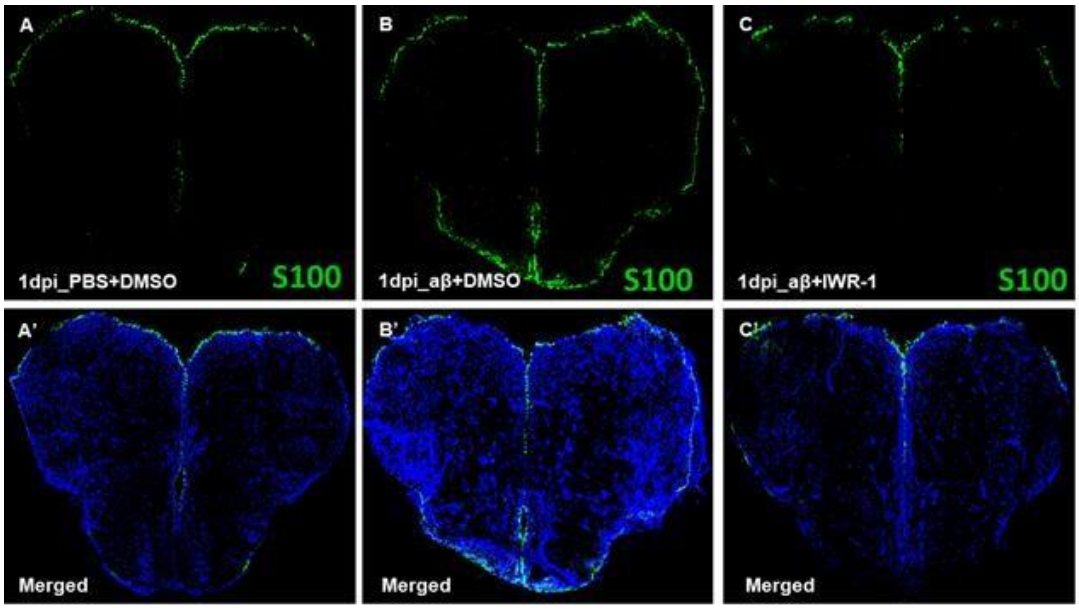

Figure 34: Anti-S100 immunofluorescence staining of 1dpi (Anti-S100 immunostaining of brain section obtained from 1dpi_PBS+DMSO (A), 1dpi_ Aβ+DMSO (B), 1dpi_ Aβ+IWR-1 (C), A' , B' , C' represent the DAPI staining. Scale bars 100µm).

RGC activation was observed in fish injected with only Aß, while a severe decrease in activation was observed in the ventral and dorsal nucleus of the telencephalic area in fish treated with IWR-1. This region is also the region where neurogenesis takes place intensively (Figure 34).

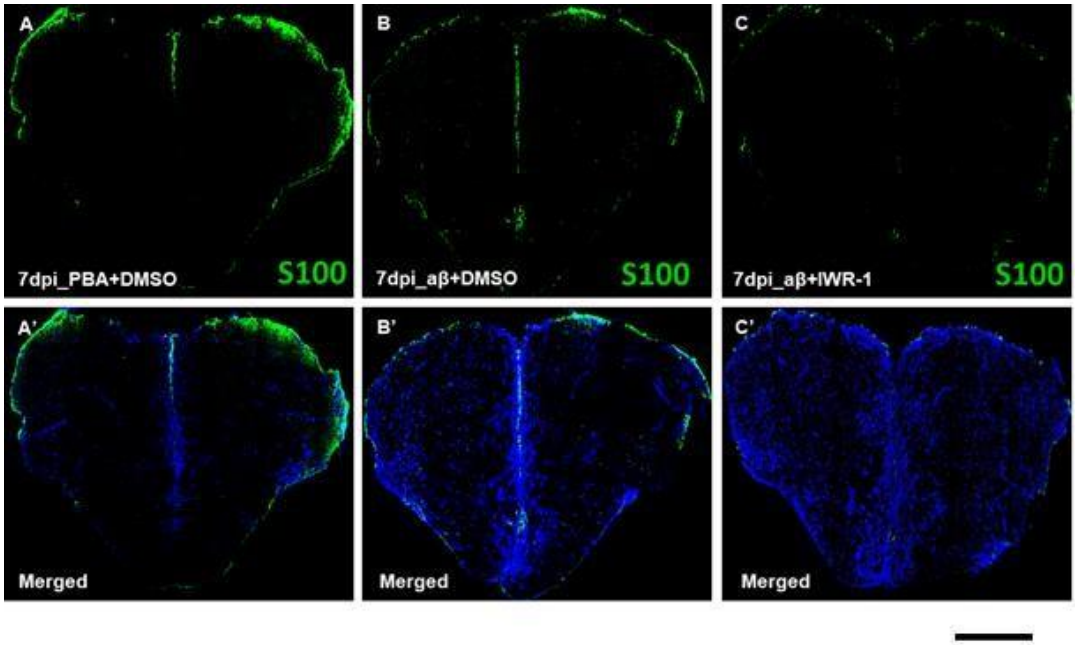

Figure 35: Anti-S100 immunofluorescence staining of 7dpi (Anti-S100 immunostaining of brain section obtained from 1-7dpi_PBS+DMSO (A), 7dpi_ Aβ+DMSO (B), 7dpi_ Aβ+IWR-1 (C), A' , B' , C' represent the DAPI staining. Scale bars 100µm).

Although the results observed at 7dpi do not mean much different from 1 dpi, the decrease in RGC activation after WNT inhibition is more evident here (Figure 35).

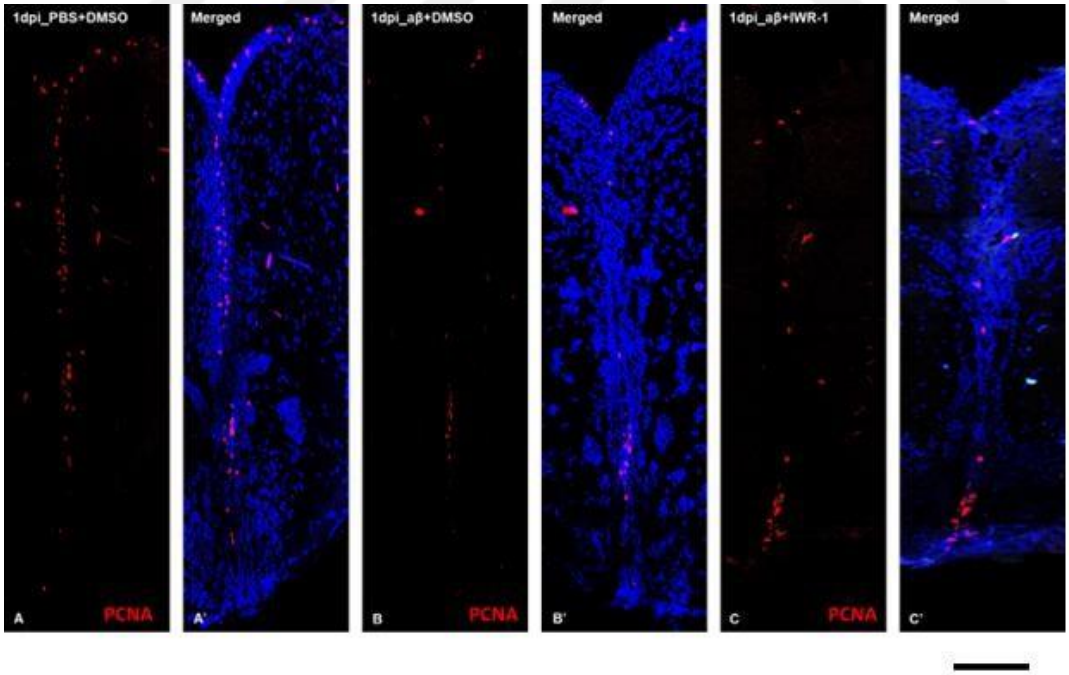

Figure 36: Anti-PCNA immunofluorescence staining of 1dpi (Anti-PCNA immunostaining of brain section obtained from 1dpi_PBS+DMSO (A), 1dpi_ Aβ+DMSO (B), 1dpi_ Aβ+IWR-1 (C), A' , B' , C' represent the DAPI staining).

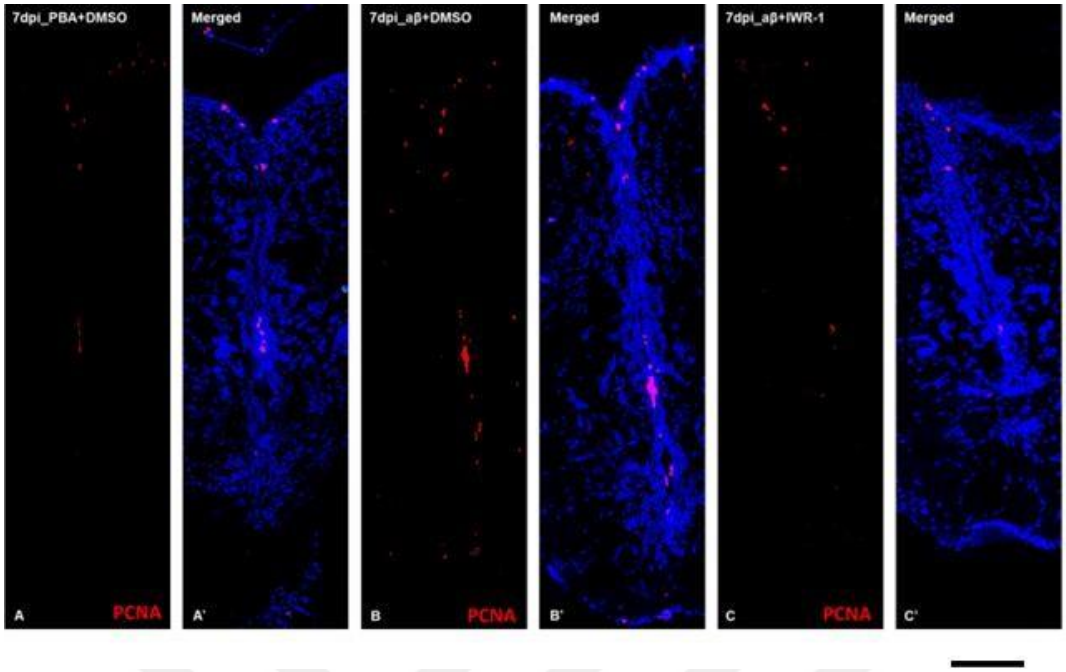

Figure 37: Anti-PCNA immunofluorescence staining of 7dpi (Anti-PCNA immunostaining of brain section obtained from 1-7dpi_PBS+DMSO (A), 7dpi_ Aβ+DMSO (B), 7dpi_ Aβ+IWR-1 (C), A' , B' , C' represent the DAPI staining. Scale bars 100µm)

Although there was no big difference in PCNA positive cell numbers of WNT activation performed at 1dpi, compared to the group injected with only Aβ; It was quite evident in the ventral/dorsal nucleus of the ventral telencephalic area, in the group that underwent IWR-1 treatment at 7dpi. According to the results, it can be said that IWR-1 treatment reduces the regenerative response, impairs the repair mechanism in the brain, and prevents the clearance of amyloid plaques (Figure 36, 37).

4. DISCUSSION

It has been proven in studies that the main cause of Alzheimer's Disease, and dementia observed in patients, is dysfunctional Aβ metabolism.

The production of neurotoxic Aβ from proteolysis of amyloid precursor proteins (APP) through enzymes is the most critical step in AD development. In this context, pharmacotherapies developed for the treatment of AD are generally aimed at providing Aβ production and clearance of aggregation. It is thought that this strategy will stop/reverse the pathological neuron loss that causes cognitive decline. By modeling Alzheimer's disease with Aβ42-toxicity to be created using Aβ42 in the adult zebrafish brain, the activation and role of Wnt/β-catenin signal transduction in various stages of disease formation and changes in the brain during Alzheimer's

disease, apoptosis and neurogenesis were investigated for the first time. Carried out in the zebrafish model, which is a creature with high neurogenesis capacity. Thus, important information was obtained not only on the emergence of the disease, but also on the repair mechanism triggered by the disease and its functioning, and the responses at different stages were analyzed comparatively at the molecular level for the first time.

This model demonstrated that (1) it inhibits aβ accumulation, (2) it triggers RGC activation and helps to clear accumulated aβ plaques, and (3) it compensates neuronal loss by triggering proliferation in the long term.

Alzheimer's disease is a disease that progresses with age. As time progresses, damage to the brain gradually increases and symptoms develop. Neurodegenerative diseases are studied with samples taken from body fluids such as blood and cerebrospinal fluid. Alzheimer's disease is a disease that progresses with age. As time progresses, damage to the brain gradually increases and symptoms develop. Neurodegenerative diseases are examined with samples taken from body fluids such as blood and cerebrospinal fluid. However, an autopsy and biopsy should be performed to understand the extent of the disease and determine the extent of brain damage and make a definitive diagnosis. As a result, it can be done by detecting pathological findings specific to AD. This requires very long periods and certain procedures. In order to understand how the pathogenesis of AD occurs, animal models have been created and the progression processes of Alzheimer's disease can be examined. The adult mammalian brain has a very limited capacity to repair damage to neuronal networks. Mammalian neurogenesis occurs through neural stem cells confined to two regions of the forebrain, namely the subventricular region of the lateral ventricles (SVZ) in the telencephalon and the subgranular region of the dentate gyrus (SGZ) in the hippocampus (Alvarez-Buylla et al., 2001; Kriegstein & Alvarez-Buylla, 2009; Bonfanti & Peretto, 2011).

Low neurogenesis capacity is accompanied by the limited potential for the integration of nascent neurons in most regions of the brain, necessitating the use of another platform without these limitations for the development of new therapeutic approaches (Bhardwaj et al., 2006; Ernst & Frisen, 2015; Alunni & Bally-Cuif, 2016). A good experimental model of Alzheimer's disease is expected to improve the clinical features and pathological and neurochemical findings of the disease. However, animal models in which human mutations that produce typical AD in humans have also been created. However, only some of these features, including the disease, can be imitated, and an animal model that contains all the features of the disease has not been

developed yet. In this study, Aβ plaques (Figure 5), which accumulate as the disease progresses, were able to mimic human AD in many ways, such as observing glial cell density (Figure 6), which is activated as a result of neuroinflammation, and neuronal loss, which can also be observed molecularly (Figure 9, 10)

6XTCF reporter lines are highly useful tools for studying Tcf/Lef-mediated Wnt/β-catenin signaling-dependent processes (Shimizu et al., 2012). Becker et al 2017; In the experimental model created in the 6XTCF line, showed that Wnt/β-catenin signaling in fibroblast-like cells at the lesion activates axon regrowth through the accumulation of Collagen XII. The inhibitory extracellular matrix at the spinal lesion site is the major obstacle to axonal regeneration in mammals. Whereas the extracellular matrix of zebrafish allows axon regrowth, and this regeneration process could be observed with the 6XTCF line. Likewise, the role of activation of Wnt/β-catenin signaling in the regulation of cellular and molecular events in the early wound healing stage, which was also performed in our laboratory, was revealed by using the transgenic 6XTCF line (Demirci et al., 2020).

GFAP, which is a marker of abnormal activation of astrocytes in neuronal damage to the brain known as astrogliosis, is also an astrocytic cell protein. It was observed that GFAP expression was correlated with Aβ plaque density in AD patients with cognitive impairment. Recent studies are investigating whether high GFAP fusion may be a clinical symptom in normal adults at risk of AD. When the results we obtained in Figure 6 are examined; GFAP increased in correlation with this at 4,7,14 dpi (Figure 5D,E,F) where Aβ plaques are most intense. It is noteworthy that in the qPCR results performed with samples obtained from mRNA, the GFAP expression level was the lowest on the 14th day when the highest Aβ accumulation was observed (Figure 6). Again, when the toxicity model we created in 6XTCFs was controlled, 7 and 14 dpi, where amyloid plaques were intense, and GFAP levels at 7 dpi showed significantly higher levels but remained under control on the 14th day. When all these results are evaluated together, although the GFAP change seen in patients has gained a dynamic structure, the high GFAP expression seen in healthy people can be considered a risk.

Activation of the WNT signaling pathway is thought to have a neuroprotective effect on AD (Alvarez et al., 2004; Quintanilla et al., 2015). Silva-Alvarez et al. (2013), Wnt-5a activation modulates mitochondrial dynamics; it has been shown that it prevents the changes induced by Aβ and compensates for the increase in BCL-2 induced by Aβ.

Considering these results and the downregulation of the Wnt signaling pathway found in

samples from previous Alzheimer's patients; our expected result was that there was an increase in Alzheimer's markers and aβ accumulation in the experimental groups in which Wnt/β-catenin was inhibited by IWR-1. As a matter of fact, upregulation was observed in the increase of Alzheimer's-related genes seen in Figure 27 (Figure 27B,C,E,F). However, no change was observed in the 1dpi APPA gene, while a significant downregulation was observed in the 7dpi APPB gene. When the literature is examined, it has been observed that an increase in the APP gene family is expected in all samples taken from AD patients and in all animal models created. Based on this conclusion, it was considered as a question mark and a limitation of this study whether Wnt activation would have an adverse effect on AD.

Despite this question mark, amyloid beta accumulations observed in the model created, a prominent increase was observed in the experimental groups treated with IWR-1, while it was observed that RGCs could not be activated in s100 staining. In PCNA staining performed at the same time, the elevation seen in the positive control group was not observed in the IWR experimental groups. Considering all these, the toxicity model created shows that the Wnt/β-Catenin signaling pathway has a key role in the RGC activation required for the inhibition and clearance of Aβ accumulation in zebrafish.

Although more results are needed to determine the precise contribution of the Wnt signaling pathway to AD pathogenesis, targeting Wnt signaling components and restoring the brain may provide new therapeutic avenues for AD.

5. CONCLUSION and FUTURE ASPECTS

Aβ plaques are a disease that leads to neuronal dysfunction, neurodegeneration, and cognitive impairment in AD, eventually leading to brain failure and death. As mentioned throughout the thesis, Wnt signaling is an important signaling pathway in the nervous system, neuronal degeneration, and regeneration processes. In this context, permanent activation of Wnt signaling will protect neurons from Aβ toxicity and is a promising therapeutic target for the treatment of the disease. Therefore, further studies are needed to fully understand the biological mechanisms underlying pathological changes in AD for Wnt signaling, and specifically for the dysfunctional Wnt signaling that occurs in AD. In addition, since Alzheimer's Disease requires long-term care, the prevention and treatment of this disease with high resource consumption is of great importance to the health system.

6. REFERENCES

Alarcón, M. A., Medina, M. A., Hu, Q., Avila, M. E., Bustos, B. I., Pérez-Palma, E., & De Ferrari, G. V. (2013). A novel functional low-density lipoprotein receptor-related protein 6 gene alternative splice variant is associated with Alzheimer's disease. *Neurobiol. Aging*, *34*(6), 1709-e9. doi: 10.1016/j.neurobiolaging.2012.11.004

Alunni, A., & Bally-Cuif, L. (2016). A comparative view of regenerative neurogenesis in vertebrates. *Development*, *143*(5), 741-753. doi: 10.1242/dev.122796

Alvarez, A. R., Godoy, J. A., Mullendorff, K., Olivares, G. H., Bronfman, M., & Inestrosa, N. C. (2004). Wnt-3a overcomes β-amyloid toxicity in rat hippocampal neurons. *Exp. Cell Res.*, *297*(1), 186-196. doi: 10.1016/j.yexcr.2004.02.028

Alvarez-Buylla, A., García-Verdugo, J. M., & Tramontin, A. D. (2001). A unified hypothesis on the lineage of neural stem cells. *Nat. Rev. Neurosci.*, *2*(4), 287-293.

Aman, A. J., Fulbright, A. N., & Parichy, D. M. (2018). Wnt/β-catenin regulates an ancient signaling network during zebrafish scale development. *Elife*, *7*, e37001. doi: 10.7554/eLife.37001

Arvanitakis, Z., Shah, R. C., & Bennett, D. A. (2019). Diagnosis and management of dementia. *Jama*, *322*(16), 1589-1599. doi: 10.1001/jama.2019.4782

Avila, R. L., Tevlin, B. R., Lees, J. P., Inouye, H., & Kirschner, D. A. (2007). Myelin structure and composition in zebrafish. *Neurochem. Res.*, *32*(2), 197-209. doi: 10.1007/s11064-006-9136-5

Azbazdar, Y., Karabicici, M., Erdal, E., & Ozhan, G. (2021). Regulation of Wnt Signaling Pathways at the Plasma Membrane and Their Misregulation in Cancer. *Front. Cell Dev. Biol.*, *9*, 631623. doi: 10.3389/fcell.2021.631623

Bai, B., Wang, X., Li, Y., Chen, P. C., Yu, K., Dey, K. K., ... & Peng, J. (2020). Deep multilayer brain proteomics identifies molecular networks in Alzheimer's disease progression. *Neuron*, *105*(6), 975-991. doi: 10.1016/j.neuron.2019.12.015

Barker, W. W., Luis, C. A., Kashuba, A., Luis, M., Harwood, D. G., Loewenstein, D., ... & Duara, R. (2002). Relative frequencies of Alzheimer disease, Lewy body, vascular and frontotemporal dementia, and hippocampal sclerosis in the State of Florida Brain Bank. *Alzheimer Dis. Assoc. Disord.*, *16*(4), 203-212.

Bhardwaj, R. D., Curtis, M. A., Spalding, K. L., Buchholz, B. A., Fink, D., Björk-Eriksson, T., ... & Frisén, J. (2006). Neocortical neurogenesis in humans is restricted to

development. *PNAS*, *103*(33), 12564-12568. doi: 10.1073/pnas.060517710

Bonfanti, L., & Peretto, P. (2011). Adult neurogenesis in mammals–a theme with many variations. *Eur. J. Neurosci.*, *34*(6), 930-950. doi: 10.1111/j.1460-9568.2011.07832.x

Bronzuoli, M. R., Iacomino, A., Steardo, L., & Scuderi, C. (2016). Targeting neuroinflammation in Alzheimer's disease. *J. Inflamm. Res.*, *9*, 199. doi: 10.2147/JIR.S86958

Cameron, D. J., Galvin, C., Alkam, T., Sidhu, H., Ellison, J., Luna, S., & Ethell, D. W. (2012). Alzheimer's-related peptide amyloid-β plays a conserved role in angiogenesis. *PLoS One*, *7*(7), e39598. doi: 10.1371/journal.pone.0039598

Caricasole, A., Copani, A., Caraci, F., Aronica, E., Rozemuller, A. J., Caruso, A., Storto, M., Gaviraghi, G., Terstappen, G. C., & Nicoletti, F. (2004). Induction of Dickkopf-1, a negative modulator of the Wnt pathway, is associated with neuronal degeneration in Alzheimer's brain. *J. Neurosci.*, *24*(26), 6021–6027

Coric, V., Salloway, S., van Dyck, C. H., Dubois, B., Andreasen, N., Brody, M., ... & Berman, R. M. (2015). Targeting prodromal Alzheimer disease with avagacestat: a randomized clinical trial. *JAMA neurology*, *72*(11), 1324-1333. doi: 10.1001/jamaneurol.2015.0607

De Ferrari, G. V., Papassotiropoulos, A., Biechele, T., De-Vrieze, F. W., Avila, M. E., Major, M. B., ... & Moon, R. T. (2007). Common genetic variation within the low-density lipoprotein receptor-related protein 6 and late-onset Alzheimer's disease. *PNAS*, *104*(22), 9434-9439. doi: 10.1073/pnas.0603523104

Demirci, Y., Cucun, G., Poyraz, Y. K., Mohammed, S., Heger, G., Papatheodorou, I., & Ozhan, G. (2020). Comparative transcriptome analysis of the regenerating zebrafish telencephalon unravels a resource with key pathways during two early stages and activation of wnt/β-catenin signaling at the early wound healing stage. *Front. Cell Dev. Biol.*, *8*, 1054. doi: 10.3389/fcell.2020.584604

Diedrich, J., Wietgrefe, S., Zupancic, M., Staskus, K., Retzel, E., Haase, A. T., & Race, R. (1987). The molecular pathogenesis of astrogliosis in scrapi and Alzheimer's disease. *Microb. Pathog.*, *2*, 435-442.

Doody, R. S., Thomas, R. G., Farlow, M., Iwatsubo, T., Vellas, B., Joffe, S., ... & Mohs, R. (2014). Phase 3 trials of solanezumab for mild-to-moderate Alzheimer's disease. *N. Engl. J. Med.*, *370*(4), 311-321. doi: 10.1056/NEJMoa1312889

Egan, M. F., Kost, J., Voss, T., Mukai, Y., Aisen, P. S., Cummings, J. L., ... & Michelson, D.

(2019). Randomized trial of verubecestat for prodromal Alzheimer's disease. *N. Engl. J. Med.*, *380*(15), 1408-1420. doi: 10.1056/NEJMoa1812840

Elliott, C., Rojo, A. I., Ribe, E., Broadstock, M., Xia, W., Morin, P., ... & Killick, R. (2018). A role for APP in Wnt signalling links synapse loss with β-amyloid production. *Transl. Psychiatry*, *8*(1), 1-13. doi: 10.1038/s41398-018-0231-6

Ernst, A., & Frisén, J. (2015). Adult neurogenesis in humans-common and unique traits in mammals. *PLoS Biol.*, *13*(1), e1002045. doi: 10.1371/journal.pbio.1002045

Glenner, G. G., & Wong, C. W. (1984). Alzheimer's disease: initial report of the purification and characterization of a novel cerebrovascular amyloid protein. *Biochem. Biophys. Res. Commun.*, *120*(3), 885-890.

Golde, T. E., Koo, E. H., Felsenstein, K. M., Osborne, B. A., & Miele, L. (2013). γ-Secretase inhibitors and modulators. *Biochim. Biophys. Acta Biomembr.*, *1828*(12), 2898-2907. doi: 10.1016/j.bbamem.2013.06.005

Gonzalez-Sancho, J. M., Aguilera, O., Garcia, J. M., Pendas-Franco, N., Pena, C., Cal, S., ... & Munoz, A. (2005). The Wnt antagonist DICKKOPF-1 gene is a downstream target of β-catenin/TCF and is downregulated in human colon cancer. *Oncogene*, *24*(6), 1098-1103. doi: 10.1038/sj.onc.1208303

Guo, S. (2004). Linking genes to brain, behavior and neurological diseases: what can we learn from zebrafish?. *Genes, Brain Behav.*, *3*(2), 63-74.

Heckmann, B. L., Teubner, B. J., Tummers, B., Boada-Romero, E., Harris, L., Yang, M., ... & Green, D. R. (2019). LC3-associated endocytosis facilitates β-amyloid clearance and mitigates neurodegeneration in murine Alzheimer's disease. *Cell*, *178*(3), 536-551. doi: 10.1016/j.cell.2019.05.056

Henley, D., Raghavan, N., Sperling, R., Aisen, P., Raman, R., & Romano, G. (2019). Preliminary Results of a Trial of Atabecestat in Preclinical Alzheimer's Disease. *N. Engl. J. Med.*, *380*(15), 1483-1485. doi: 10.1056/nejmc1813435

Hippius, H., & Neundörfer, G. (2003). The discovery of Alzheimer's disease. *Dialogues Clin. Neurosci.*, *5*(1), 101. doi: 10.31887/DCNS.2003.5.1/hhippius

Jack Jr, C. R., Bennett, D. A., Blennow, K., Carrillo, M. C., Dunn, B., Haeberlein, S. B., ... & Silverberg, N. (2018). NIA-AA research framework: toward a biological definition of Alzheimer's disease. *Alzheimers. Dement.*, *14*(4), 535-562. doi: 10.1016/j.jalz.2018.02.018

Jho, E. H., Zhang, T., Domon, C., Joo, C. K., Freund, J. N., & Costantini, F. (2002). Wnt/β-catenin/Tcf signaling induces the transcription of Axin2, a negative regulator of the signaling pathway. *Mol. Cell. Biol., 22*(4), 1172-1183. doi: 10.1128/MCB.22.4.1172-1183.2002

Karran, E., Mercken, M., & De Strooper, B. (2011). The amyloid cascade hypothesis for Alzheimer's disease: an appraisal for the development of therapeutics. *Nat. Rev. Drug Discov., 10*(9), 698-712. doi: 10.1038/nrd3505

Kawai, H., Arata, N., & Nakayasu, H. (2001). Three-dimensional distribution of astrocytes in zebrafish spinal cord. *Glia*, 36, 406-413.

Kawamura, N., Takaoka, K., Hamada, H., Hadjantonakis, A. K., Sun-Wada, G. H., & Wada, Y. (2020). Rab7-Mediated Endocytosis Establishes Patterning of Wnt Activity through Inactivation of Dkk Antagonism. *Cell Rep., 31*(10), 107733. doi: 10.1016/j.celrep.2020.107733

Kitazawa, M., Medeiros, R., & M La Ferla, F. (2012). Transgenic mouse models of Alzheimer disease: developing a better model as a tool for therapeutic interventions. *Curr. Pharm. Des., 18*(8), 1131-1147. doi: 10.2174/138161212799315786

Koulen, P., Janowitz, T., Johnston, L. D., & Ehrlich, B. E. (2000). Conservation of localization patterns of IP (3) receptor type 1 in cerebellar Purkinje cells across vertebrate species. *J Neurosci Res.*, 61, 493-499.

Kriegstein, A., & Alvarez-Buylla, A. (2009). The glial nature of embryonic and adult neural stem cells. *Annu. Rev. Neurosci., 32,* 149-184. doi: 10.1146/annurev.neuro.051508.135600

Kumari, U., & Heese, K. (2010). Cardiovascular dementia-a different perspective. *Open Biochem. J., 4*, 29. doi: 10.2174/1874091X01004010029

La Ferla, F. M., & Green, K. N. (2012). Animal models of Alzheimer disease. *Cold Spring Harb. Perspect. Med., 2*(11), a006320. doi: 10.1101/cshperspect.a006320

La Ferla, F. M., Green, K. N., & Oddo, S. (2007). Intracellular amyloid-β in Alzheimer's disease. *Nat. Rev. Neurosci., 8*(7), 499-509. doi: 10.1038/nrn2168

Liu, Z., Li, T., Li, P., Wei, N., Zhao, Z., Liang, H., ... & Wei, J. (2015). The ambiguous relationship of oxidative stress, tau hyperphosphorylation, and autophagy dysfunction in Alzheimer's disease. *Oxid. Med. Cell. Longev., 2015*. doi: 10.1155/2015/352723

Lopez, C. L., Tariot, P. N., Caputo, A., Langbaum, J. B., Liu, F., Riviere, M. E., ... & Reiman,

E. M. (2019). The Alzheimer's Prevention Initiative Generation Program: study design of two randomized controlled trials for individuals at risk for clinical onset of Alzheimer's disease. *Alzheimer's Dement.: Transl. Res. Clin. Interv.*, *5*, 216-227. doi: 10.1016/j.trci.2019.02.005

Mawuenyega, K. G., Sigurdson, W., Ovod, V., Munsell, L., Kasten, T., Morris, J. C., ... & Bateman, R. J. (2010). Decreased clearance of CNS β-amyloid in Alzheimer's disease. *Science*, *330*(6012), 1774-1774. doi: 10.1126/science.1197623

Mueller, M. V., Weizsacker, E. V., & Campos-Ortega, J. A. (1996). Expression domains of a zebrafish homologue of the Drosophila pair-rule gene hairy correspond to primordia of alternating somites. *Development*, *122*(7), 2071-2078.

Mueller, T., & Wullimann, M. F. (2009). An evolutionary interpretation of teleostean forebrain anatomy. *Brain Behav. Evol.*, *74*(1), 30-42. doi: 10.1159/000229011

Mueller, T., Vernier, P., & Wullimann, M. F. (2004). The adult central nervous cholinergic system of a neurogenetic model animal, the zebrafish *Danio rerio*. *Brain Res.*, *1011*(2), 156-169. doi: 10.1016/j.brainres.2004.02.073

Ng, L. F., Kaur, P., Bunnag, N., Suresh, J., Sung, I. C. H., Tan, Q. H., ... & Tolwinski, N. S. (2019). WNT signaling in disease. *Cells*, *8*(8), 826. doi: 10.3390/cells8080826

Niehrs C. (2006). Function and biological roles of the Dickkopf family of Wnt modulators. *Oncogene*, *25*(57), 7469–7481. doi: 10.1038/sj.onc.1210054

Ozhan, G., & Weidinger, G. Restoring tissue homeostasis: wnt signaling in tissue regeneration after acute injury. In: Hoppler S. P., Moon R. T., editors. Wnt Signalling in Development and Disease: Molecular Mechanisms and Biological Functions. Hoboken, NJ: Wiley-Blackwell; 2014. p. 339–356.

Ozhan, G., & Weidinger, G. (2015). Wnt/β-catenin signaling in heart regeneration. *Cell Regen.*, *4*(1), 4-3. doi: 10.1186/s13619-015-0017-8

Panula, P., Sallinen, V., Sundvik, M., Kolehmainen, J., Torkko, V., Tiittula, A., Moshnyakov, M., & Podlasz. P. (2006). Modulatory neurotransmitter systems and behavior: towards zebrafish models of neurodegenerative diseases. *Zebrafish*, 3, 235-247. doi: 10.1089/zeb.2006.3.235

Panza, F., Lozupone, M., Solfrizzi, V., Sardone, R., Piccininni, C., Dibello, V., ... & Imbimbo, B. P. (2018). BACE inhibitors in clinical development for the treatment of Alzheimer's disease. *Expert Rev. Neurother.*, *18*(11), 847-857. doi: 10.1080/14737175.2018.1531706

Park, E., Lee, Y., Kim, Y., & Lee, C. J. (2008). Cholinergic modulation of neural activity in the telencephalon of the zebrafish. *Neurosci Lett.*, 439, 79-83. doi: 10.1016/j.neulet.2008.04.064

Pei, J. J., Braak, E., Braak, H., Grundke-Iqbal, I., Iqbal, K., Winblad, B., & Cowburn, R. F. (1999). Distribution of active glycogen synthase kinase 3β (GSK-3β) in brains staged for Alzheimer disease neurofibrillary changes. *J. Neuropathol. Exp. Neurol.*, *58*(9), 1010-1019. doi: 10.1097/00005072-199909000-00011

Peri, F., & Nusslein-Volhard, C. (2008). Live imaging of neuronal degradation by microglia reveals a role for v0-ATPase a1 in phagosomal fusion in vivo. *Cell*, 133, 916-927. doi: 10.1016/j.cell.2008.04.037

Peters, F., Salihoglu, H., Rodrigues, E., Herzog, E., Blume, T., Filser, S., ... & Herms, J. (2018). BACE1 inhibition more effectively suppresses initiation than progression of β-amyloid pathology. *Acta Neuropathol.*, *135*(5), 695-710. doi: 10.1007/s00401-017-1804-9

Quintanilla, D., Hagemann, T., Hansen, K., & Gernaey, K. V. (2015). Fungal morphology in industrial enzyme production-modelling and monitoring. *Adv. Biochem. Engin./Biotechnol.*, 149, 29-54. doi: 10.1007/10_2015_309

Rico, E. P., Rosemberg, D. B., Seibt, K. J., Capiotti, K. M., Da Silva, R. S., & Bonan, C. D. (2011). Zebrafish neurotransmitter systems as potential pharmacological and toxicological targets. *Neurotoxicol. Teratol.*, *33*(6), 608-617. doi: 10.1016/j.ntt.2011.07.007

Rink, E., & Wullimann, M. F. (2004). Connections of the ventral telencephalon (subpallium) in the zebrafish (*Danio rerio*). *Brain Res.*, *1011*(2), 206-220. doi: 10.1016/j.brainres.2004.03.027

Rosi, M. C., Luccarini, I., Grossi, C., Fiorentini, A., Spillantini, M. G., Prisco, A., ... & Casamenti, F. (2010). Increased Dickkopf-1 expression in transgenic mouse models of neurodegenerative disease. *J. Neurochem.*, 112(6), 1539-1551. doi: 10.1111/j.1471-4159.2009.06566.x

Selkoe, D. J., & Hardy, J. (2016). The amyloid hypothesis of Alzheimer's disease at 25 years. *EMBO Mol. Med.*, *8*(6), 595-608. doi: 10.15252/emmm.201606210

Serrano-Pozo, A., Frosch, M. P., Masliah, E., & Hyman, B. T. (2011). Neuropathological alterations in Alzheimer disease. *Cold Spring Harb. Perspect. Med.*, *1*(1), a006189. doi: 10.1101/cshperspect.a006189

Shimizu, N., Kawakami, K., & Ishitani, T. (2012). Visualization and exploration of Tcf/Lef function using a highly responsive Wnt/β-catenin signaling-reporter transgenic zebrafish. *Dev. Biol.*, *370*(1), 71-85. doi: 10.1016/j.ydbio.2012.07.016

Silva-Alvarez, C., Arrázola, M. S., Godoy, J. A., Ordenes, D., & Inestrosa, N. C. (2013). Canonical Wnt signaling protects hippocampal neurons from Aβ oligomers: role of non-canonical Wnt-5a/Ca2+ in mitochondrial dynamics. *Front. Cell. Neurosci.*, *7*, 97. doi: 10.3389/fncel.2013.00097

Wagner, L. K., Gilling, K. E., Schormann, E., Kloetzel, P. M., Heppner, F. L., Krüger, E., & Prokop, S. (2017). Immunoproteasome deficiency alters microglial cytokine response and improves cognitive deficits in Alzheimer's disease-like APPPS1 mice. *Acta Neuropathol. Commun.*, *5*(1), 1-16. doi: 10.1186/s40478-017-0453-5

Wang, W. Y., Tan, M. S., Yu, J. T., & Tan, L. (2015). Role of pro-inflammatory cytokines released from microglia in Alzheimer's disease. *Ann. Transl. Med.*, *3*(10), 136. doi: 10.3978/j.issn.2305-5839.2015.03.49

Westerfield, M., McMurray, J. V., & Eisen, J. S. (1986). Identified motoneurons and their innervation of axial muscles in the zebrafish. *J. Neurosci.*, 6, 2267-2277. doi: 10.1523/JNEUROSCI.06-08-02267.1986

Xu, M., Peng, Y., Zhu, L., Wang, S., Ji, J., & Rakesh, K. P. (2019). Triazole derivatives as inhibitors of Alzheimer's disease: Current developments and structure-activity relationships. *Eur. J. Med. Chem.*, *180*, 656-672. doi: 10.1016/j.ejmech.2019.07.059

Yamamoto, S., Nishimura, O., Misaki, K., Nishita, M., Minami, Y., Yonemura, S., ... & Sasaki, H. (2008). Cthrc1 selectively activates the planar cell polarity pathway of Wnt signaling by stabilizing the Wnt-receptor complex. *Dev. Cell*, *15*(1), 23-36. doi: 10.1016/j.devcel.2008.05.007

Yoshida, M., & Macklin, W. B. (2005). Oligodendrocyte development and myelination in GFP-transgenic zebrafish. *J. Neurosci. Res.*, 81, 1-8. doi: 10.1002/jnr.20516

Zhang J., Price J. O., Graham D. G. & Montine T. J. (1998) Secondary excitotoxicity contributes to dopamine-induced apoptosis of dopaminergic neuronal cultures. *Biochem. Biophys. Res. Commun., 248*, 812-816. doi: 10.1006/bbrc.1998.9044

Zhang, F., Li, Z., Zhang, B., Du, H., Wang, B., & Zhang, X. (2019). Multi-modal deep learning model for auxiliary diagnosis of Alzheimer's disease. *Neurocomputing*, *361*, 185-195. doi: 10.1016/j.neucom.2019.04.093

7. APPENDIX

7.1. Research Ethics Committee Approval

İZMİR BİYOTIP VE GENOM MERKEZİ
HAYVAN DENEYLERİ YEREL ETİK KURULU (İBG-HADYEK)
KARARI

Toplantı Tarihi	: 14/07/2021	**Toplantı Günü**	: Çarşamba
Toplantı Sayısı	: 9	**Toplantı Saati**	: 15:30

Sayın Doçent Doktor Güneş ÖZHAN,

2021-015 Protokol No'lu; yürütücüsü olduğunuz "Alzheimer hastalığı gelişiminde Wnt/β-katenin sinyal iletiminin rolünün zebrabalığı amiloid-β toksisite modelinde araştırılması" başlıklı projenin uygulanmasında etik açıdan sakınca olmadığına oy birliği ile karar verilmiştir.

Bilgilerinizi ve gereğini rica ederiz.

(Proje Yürütücüsü) **Doç. Dr. Güneş ÖZHAN** **Başkan** (Katılmadı)	**Vet. Hek. Kerem ESMEN** **Başkan Yardımcısı**
Prof. Dr. Ensari GÜNELİ **Üye**	**Doç. Dr. Kasım DİRİL** **Üye**
Dr. Öğr. Üyesi Ayşe Banu DEMİR **Üye**	**Dr. Gülçin ÇAKAN AKDOĞAN** **Üye**
Vet. Hek. Umur KELEŞ **Üye**	**Vet. Hek. Ceren ÜLKER** **Üye** (Katılmadı)
Vet. Hek. Gizem ARALAN **Üye**	**İrem KARADAŞ** **Üye** (Katılmadı)

7.2. Curriculum Vitae

ADI SOYADI: MAKBULE DİLEK NAZLI

TC Kimlik No / Pasaport No:	
Doğum Yılı:	
Yazışma Adresi :	
Telefon :	5
Faks :	
e-posta :	

EĞİTİM BİLGİLERİ

Ülke	Üniversite	Fakülte/Enstitü	Öğrenim Alanı	Derece	Mezuniyet Yılı
Kuzey Kıbrıs Türk Cumhuriyeti	Doğu Akdeniz Üniversitesi	Fen ve Edebiyat Fakültesi	Moleküler Biyoloji ve Genetik	Lisans	2020
Türkiye	9 Eylül Üniversitesi	İzmir Uluslararası Biyotıp ve Genom Enstitüsü	Moleküler Biyoloji ve Genetik	Yüksek Lisans	2022

AKADEMİK/MESLEKTE DENEYİM

Kurum/Kuruluş	Ülke	Şehir	Bölüm/Birim	Görev Türü	Görev Dönemi
İskenderun Teknik Üniversitesi	Türkiye	HATAY	Moleküler Genetik	Stajyer	Haziran 2018-Ağustos 2018
Mustafa Kemal Üniversitesi	Türkiye	HATAY	Tıp Fakültesi	Stajyer	Ocak 2019-Şubat 2019
Mersin Üniversitesi	Türkiye	MERSİN	Mikrobiyoloji	Stajyer	Haziran 2019-Ağustos 2019
Dokuz Eylül Üniversitesi	Türkiye	İZMİR	Moleküler Biyoloji ve Genetik	Yüksek Lisans Öğrencisi	Eylül 2020-Haziran 2022

UZMANLIK ALANLARI

Uzmanlık Alanları
Moleküler Biyoloji, Alzheimer Hastalığı, Gelişim Biyolojisi, Zebra Balığı

DİĞER AKADEMİK FAALİYETLER

Son Bir Yılda Uluslararası İndekslere Kayıtlı Makale/Derleme İçin Yapılan Danışmanlık Sayısı			
Son Bir Yılda Projeler İçin Yapılan Danışmanlık Sayısı			
Yayınlara Alınan Toplam Atıf Sayısı			
Danışmanlık Yapılan Öğrenci Sayısı		**Tamamlanan**	**Devam Eden**
	Yüksek Lisans		
	Doktora		
	Uzmanlık		
Diğer Faaliyetler (Eser/görev/faaliyet/ sorumluluk/olay/üyelik vb.)			

ÖDÜLLER

Ödülün Adı	Alındığı Kuruluş	Yılı
2210/C Yurt İçi Öncelikli Alanlar Yüksek Lisans Burs Programı	TUBITAK	2021

YAYINLARI

SCI, SSCI, AHCI indekslerine giren dergilerde yayınlanan makaleler

Yabalak, E., Erdoğan-Eliuz, E. A., & **Nazlı, M. D**. (2021). Evaluation of Citrus reticulata essential oil: Chemical composition and antibacterial effectiveness incorporated gelatin on *E. coli* and *S. aureus. International Journal of Environmental Health Research*, 32, (6), 1261-1270.

Diğer dergilerde yayınlanan makaleler

Hakemli konferans/sempozyumların bildiri kitaplarında yer alan yayınlar

Tollu, G., Erdoğan-Eliuz, E. A. & **Nazlı, M. D**. (2019). The Researches Of Efficacy Of Gelatın Fılm Solutıons Incorporated Wıth Ampıcıllın Agaınst Staphylococcus Aureus And Escherıchıa Colı Bacterıa, Tam Metin Bildiri, Uluslararası Mersin Sempozyumu, 31 October 2019- 02 November 2019.

Erdoğan-Eliuz, E. A., Tollu, G., & **Nazlı, M. D**. (2019). Efficacy Of Gelatin Film Solutions Incorporated With Thymus Vulgaris And Cuminum Cyminum Against Staphylococcus Aureus, Tam Metin Bildiri, Uluslararası Mersin Sempozyumu, 31 Ekim 2019-02 Kasım 2020.
Poyraz, Y. K., Topal, G. R., **Nazlı, M. D**., Şahin, E. T., Küçüktürkmen, B., Öz, U. C., Bozkir, A., & Özhan, H. G. (2022). Trial of new drug treatments in Alzheimer's Disease model induced by Aß toxicity in zebrafish, Sözlü Sunum, 8th Internation Congress of Molecular Biology Association of Turkey, 09-12 June 2022.
İpekgil, D., **Nazlı, M. D**., Poyraz, Y. K., İşcan, E., Şahin, E. T., & Özhan, H. G. (2022). Investigation of the role of p75NTR homolog Nradd during degeneration and regeneration responses in Alzheimer?s disease in a zebrafish model of amyloidß42 toxicity, Poster Sunumu, 8th Molecular Biology Association of Turkey, 09-12 June 2022.
Azbazdar, A. Y., Poyraz, Y. K., Özalp, Ö., **Nazlı, M. D**., Cucun, G., & Özhan, H. G. (2022). High-fat diet triggers regenerative response and Wnt/ß-catenin signaling activation in the brain, Poster Sunumu, 8th Internation Congress of Molecular Biology Association of Turkey, 09-12 June 2022.